Supplementary material to the manuscript

Functionalization of $[Re_6Q_8(CN)_6]^{4-}$ Clusters by Methylation of Cyanide Ligands

Maksim A. Mikhaylov,[†] Alina D. Mironova,[†] Konstantin A. Brylev,[†,‡] Taisiya S. Sukhikh,[†,‡] Ilia V. Eltsov,[‡] Dmitri V. Stass,[§,‡], Artem L. Gushchin,[†] Noboru Kitamura,[#] and Maxim N. Sokolov*[,†,‡]

[†]Nikolaev Institute of Inorganic Chemistry SB RAS, Prospekt Akademika Lavrentyeva 3, 630090 Novosibirsk, Russia

[‡]Novosibirsk State University, ul. Pirogova 2, 630090 Novosibirsk, Russia

[§]Voevodsky Institute of Chemical Kinetics and Combustion SB RAS, ul. Institutskaya 3, 630090 Novosibirsk, Russia

[#]Department of Chemistry, Faculty of Science, Hokkaido University, 060-0810 Sapporo, Japan

(a) ^{1}H NMR

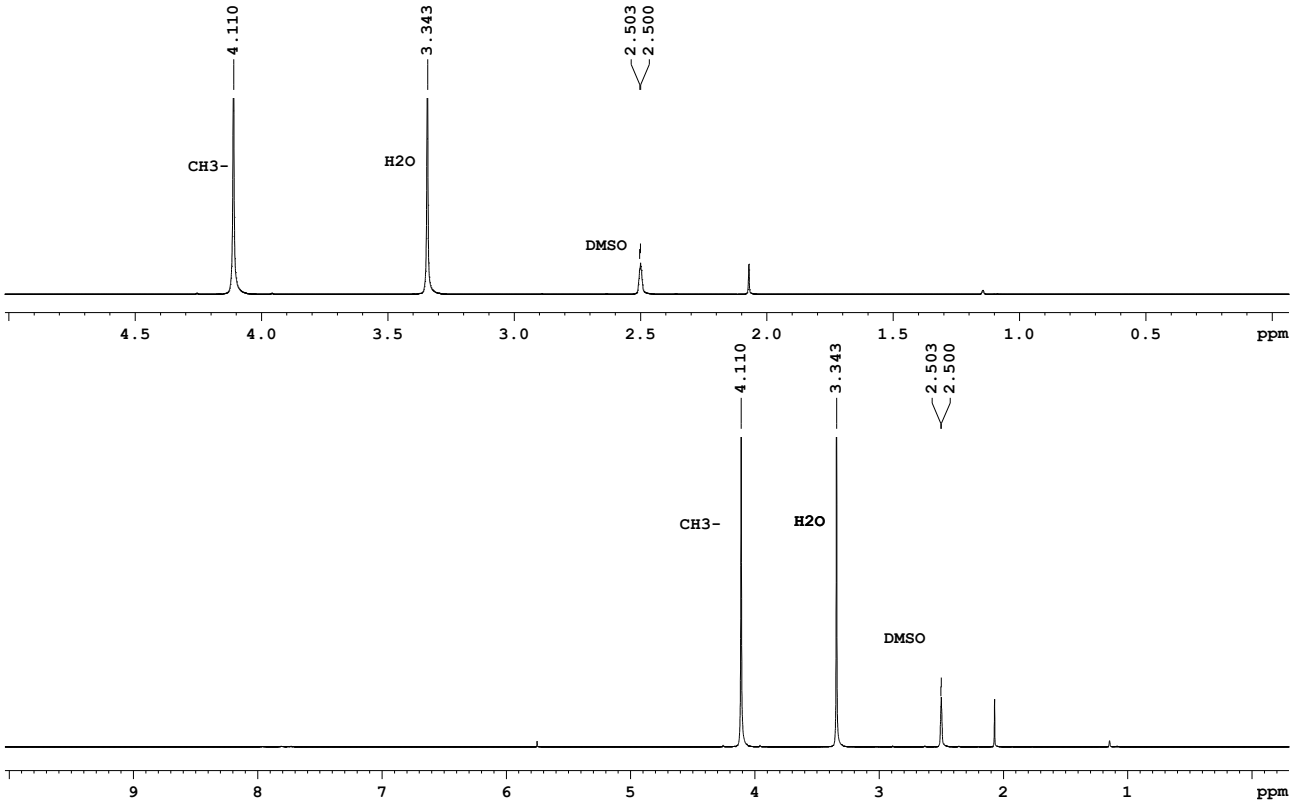

(b) ^{13}C NMR

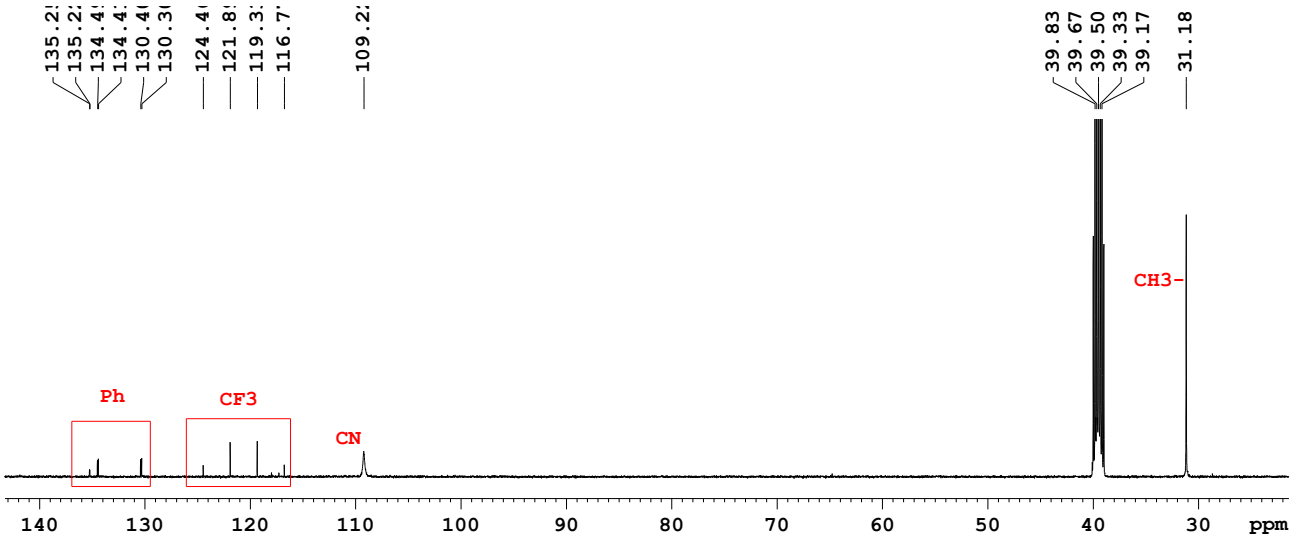

(c) $^{1}H,^{13}C$-HMBC spectrum

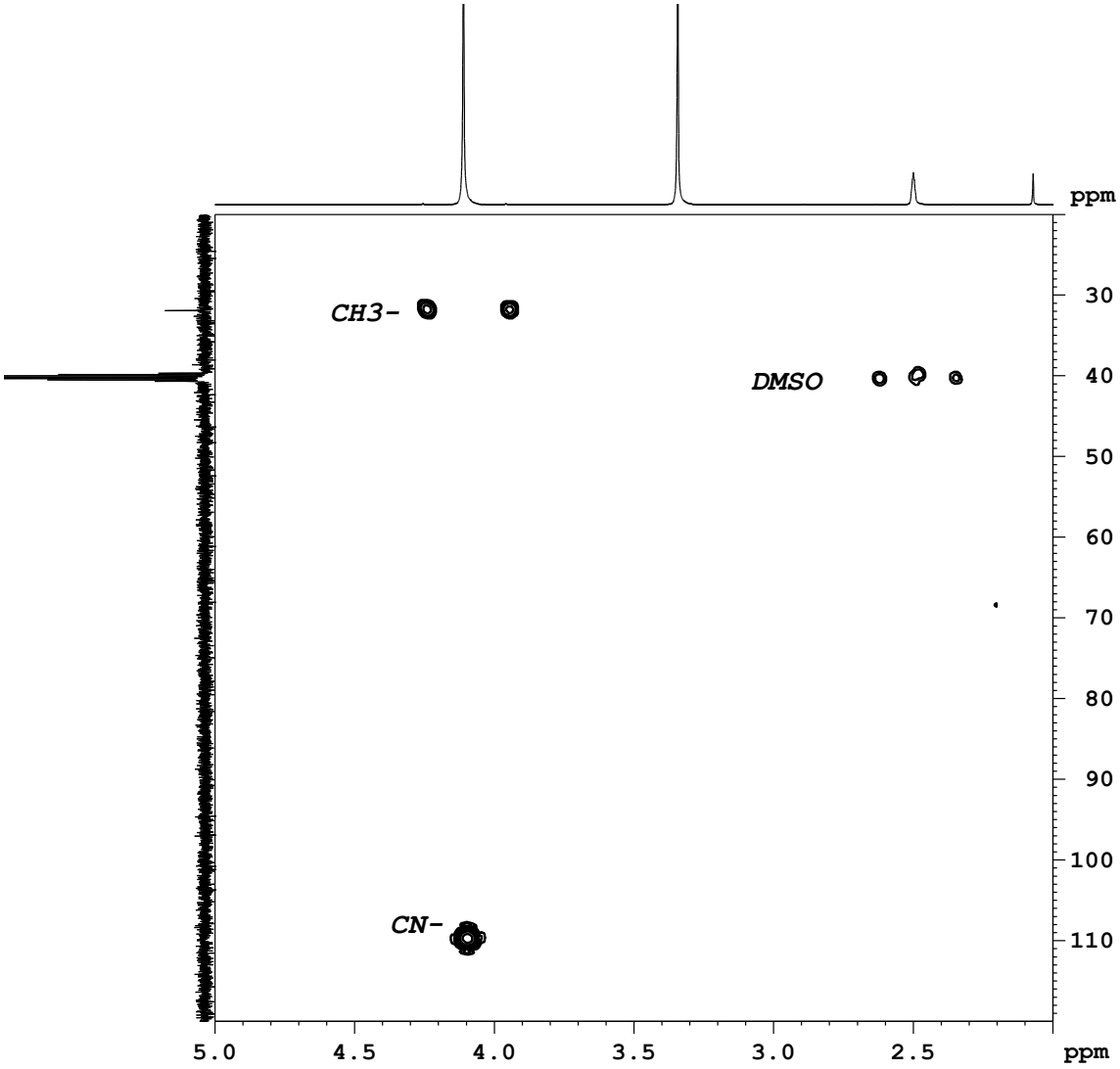

Figure S1. ^{1}H (a), ^{13}C (b) and $^{1}H,^{13}C$-HMBC (c) NMR spectra of $[Re_6S_8(CNCH_3)_6](CF_3SO_3)_2$.

(a) ^{1}H NMR

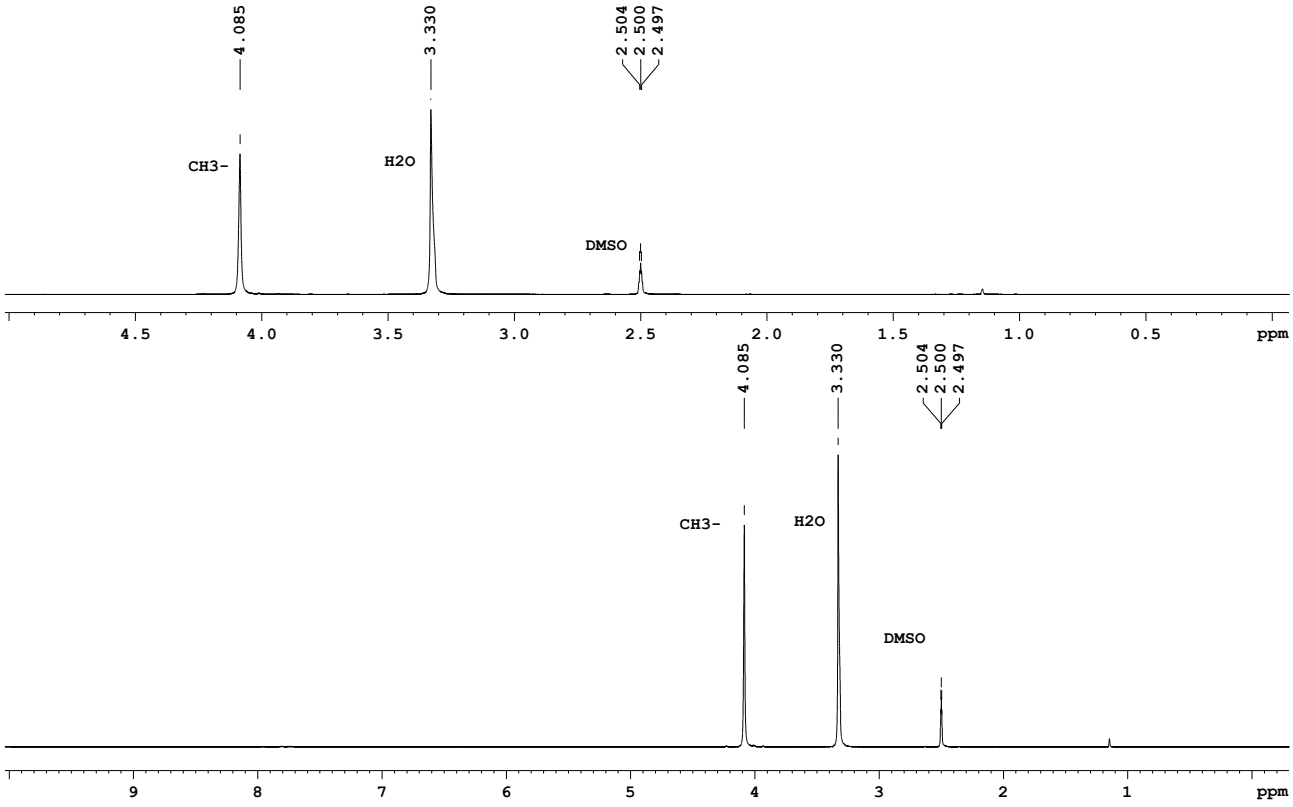

(b) ^{13}C NMR

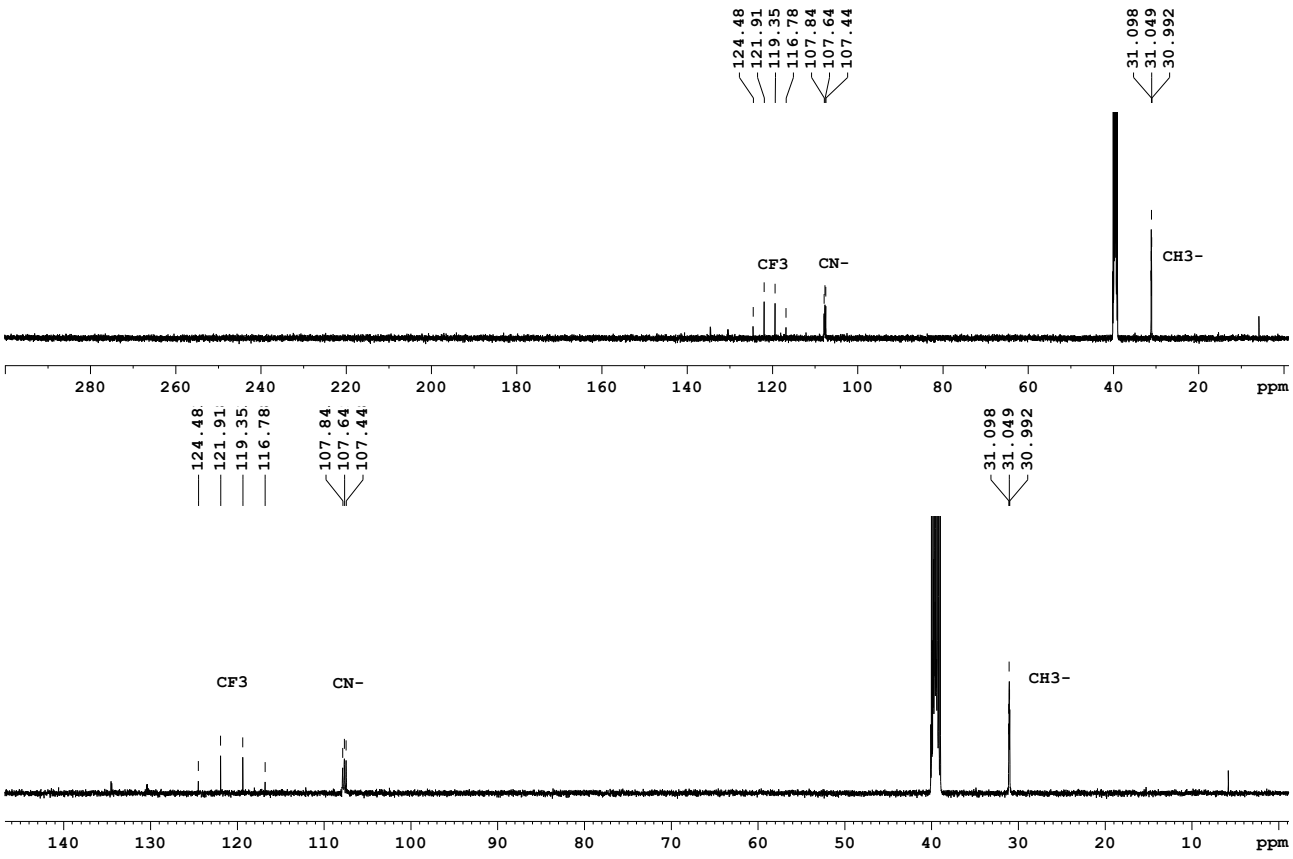

(c) ^{13}C NMR

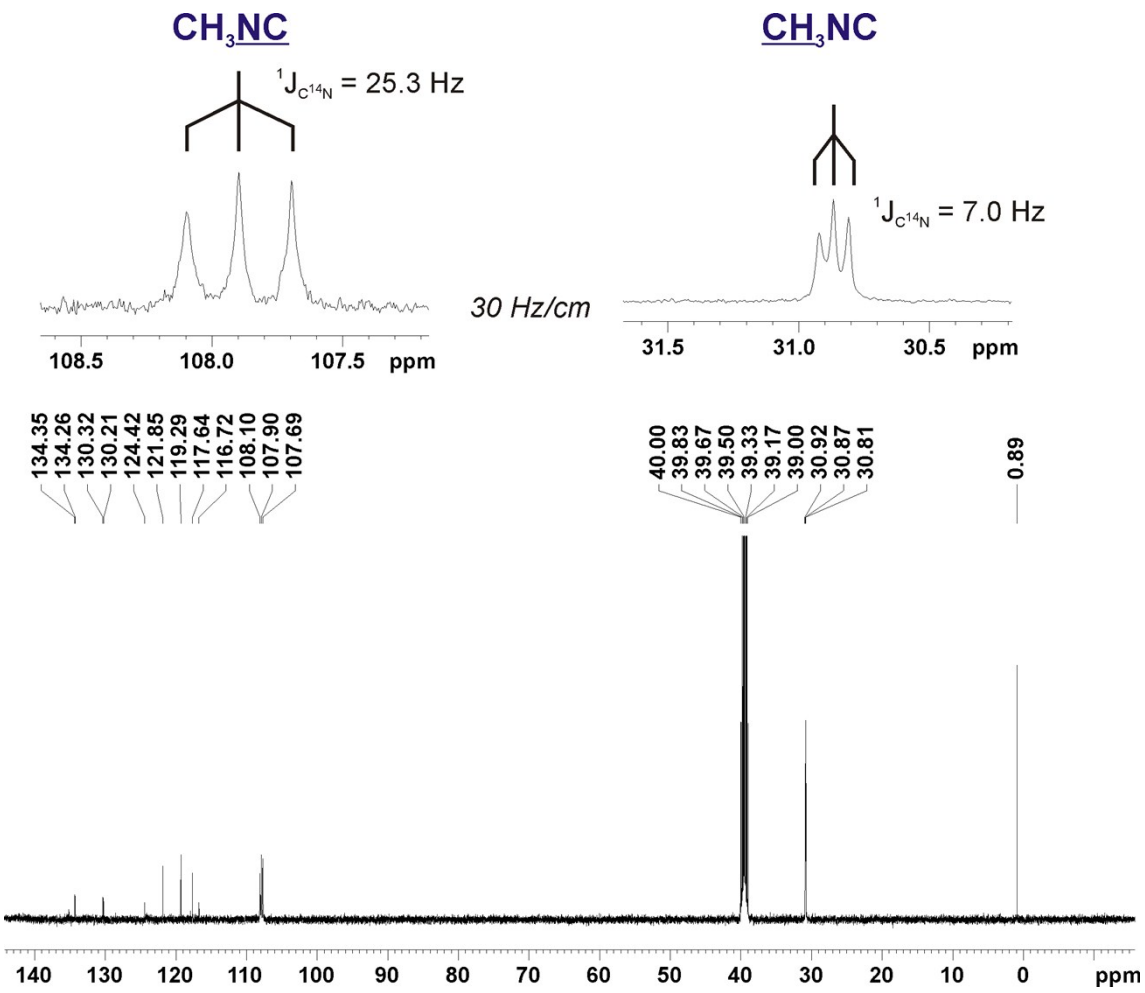

(d) ^{77}Se NMR

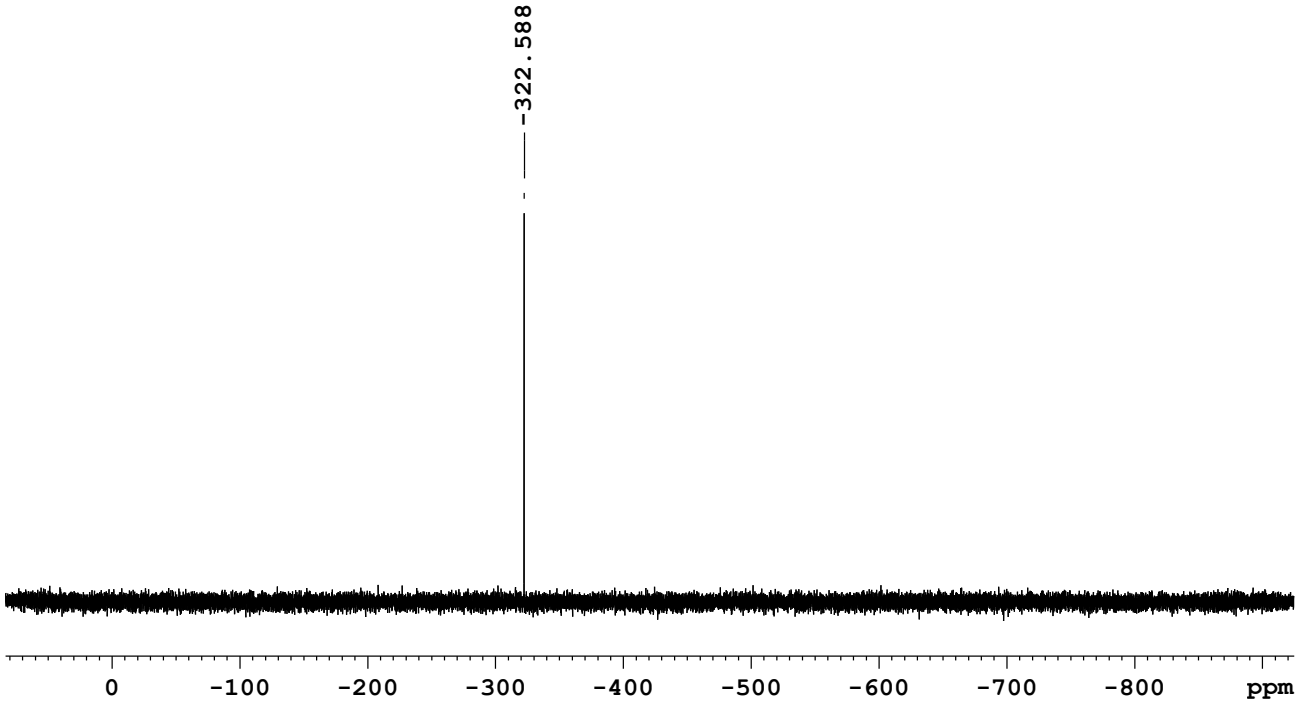

(e) ^{14}N NMR

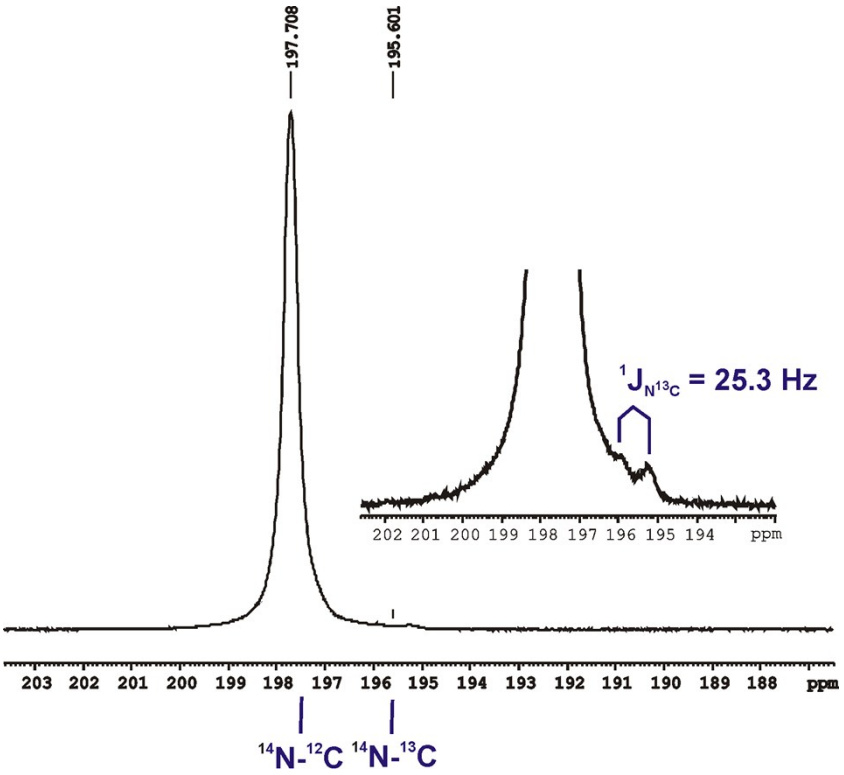

(f) ^{15}N NMR

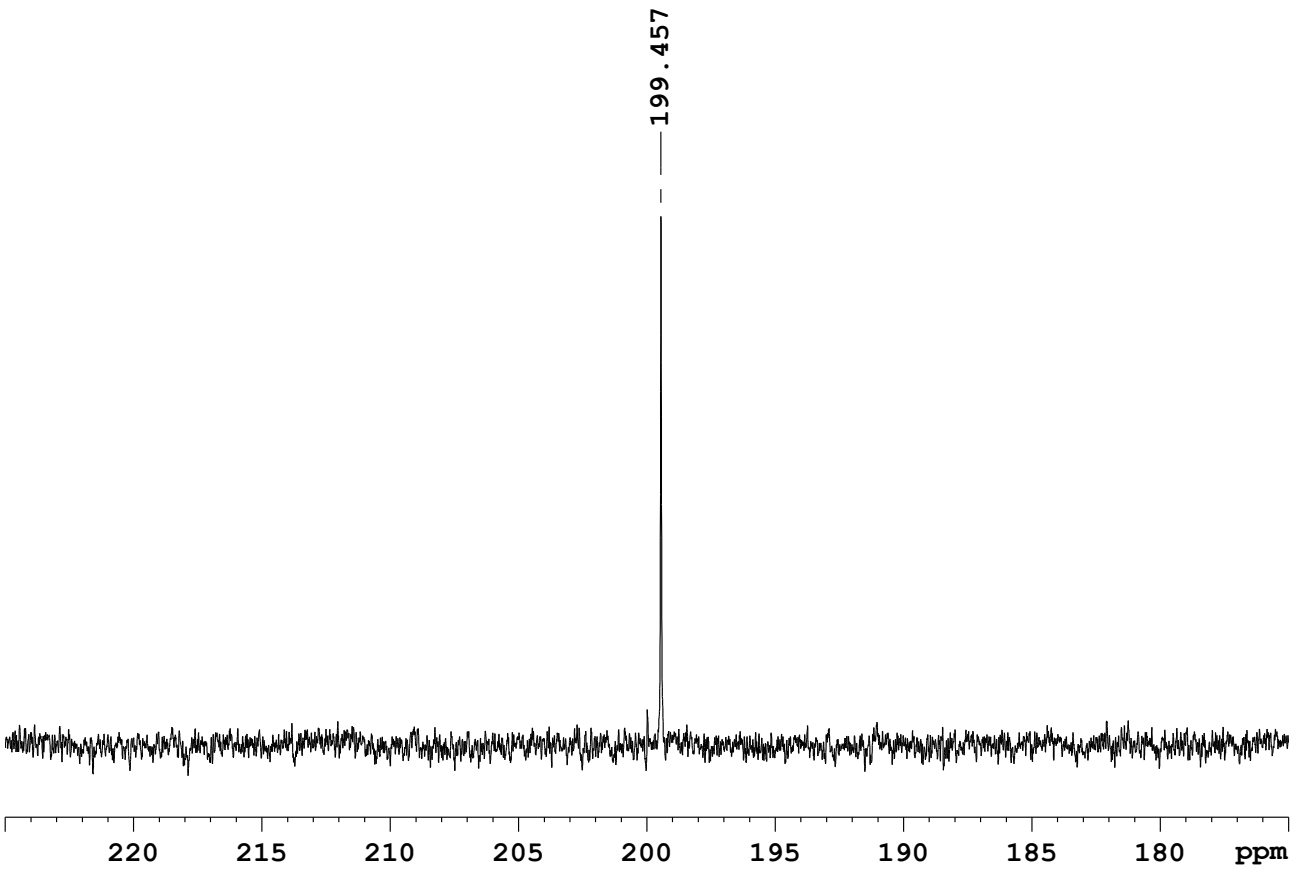

(g) $^{1}H,^{13}C$-HMBC (black) and $^{1}H,^{13}C$-HSQC (red) 2D spectra

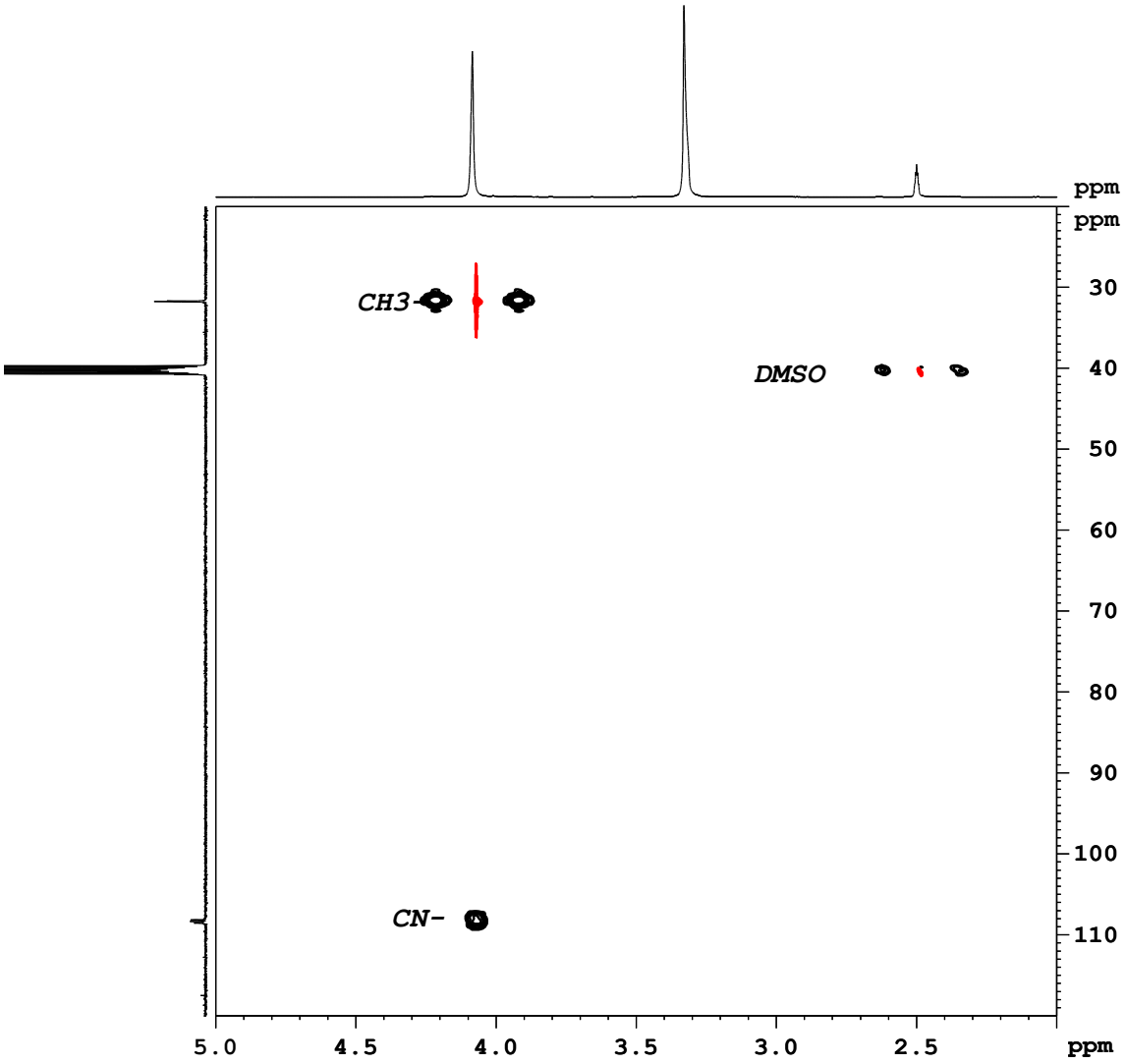

Figure S2. ^{1}H (a), ^{13}C (b,c), ^{77}Se (d), ^{14}N (e), ^{15}N (f) as well as $^{1}H,^{13}C$-HMBC and $^{1}H,^{13}C$-HSQC (g) NMR spectra of $[Re_6Se_8(CNCH_3)_6](CF_3SO_3)_2$.

(a) ^{1}H NMR

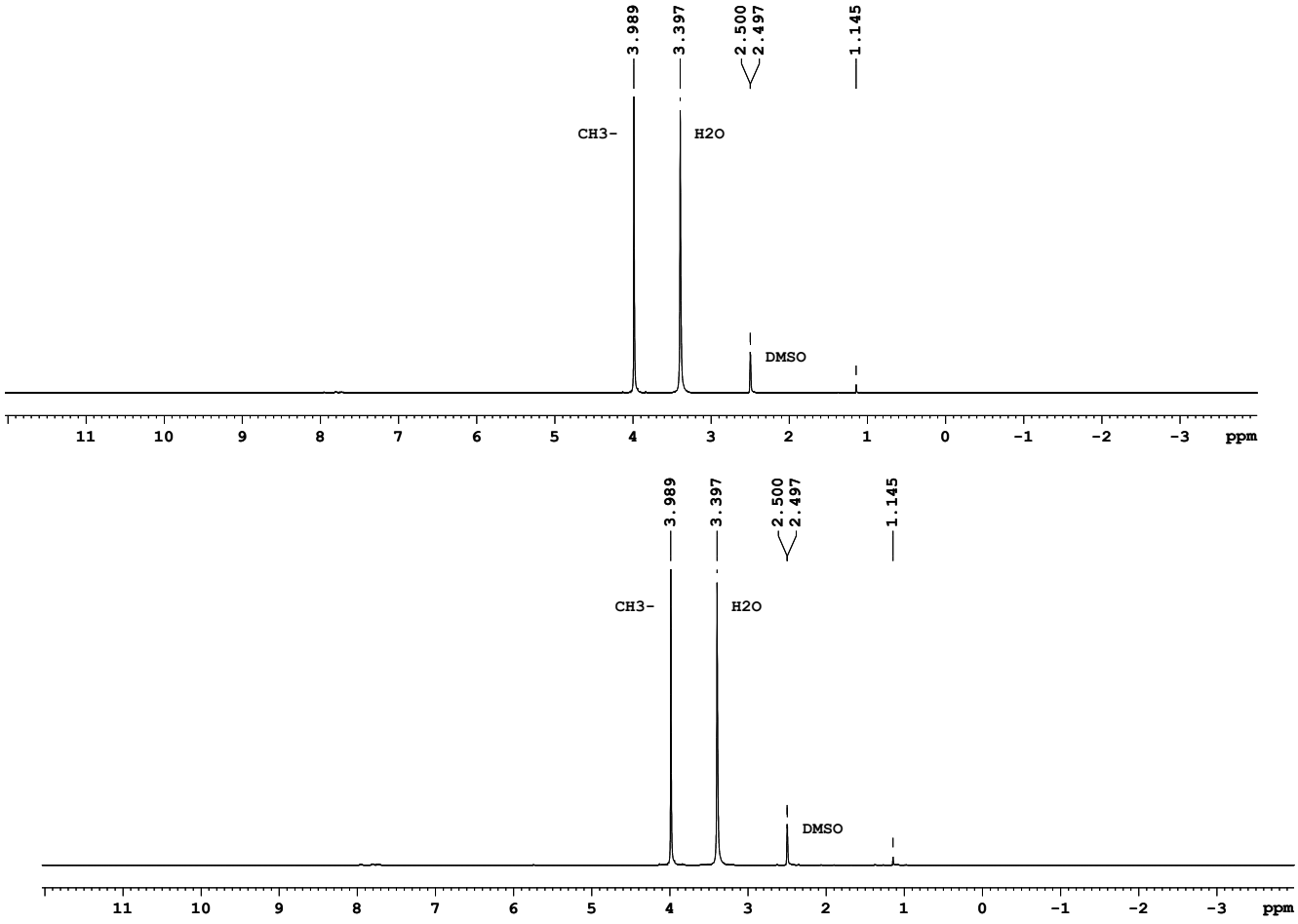

(b) ^{13}C NMR

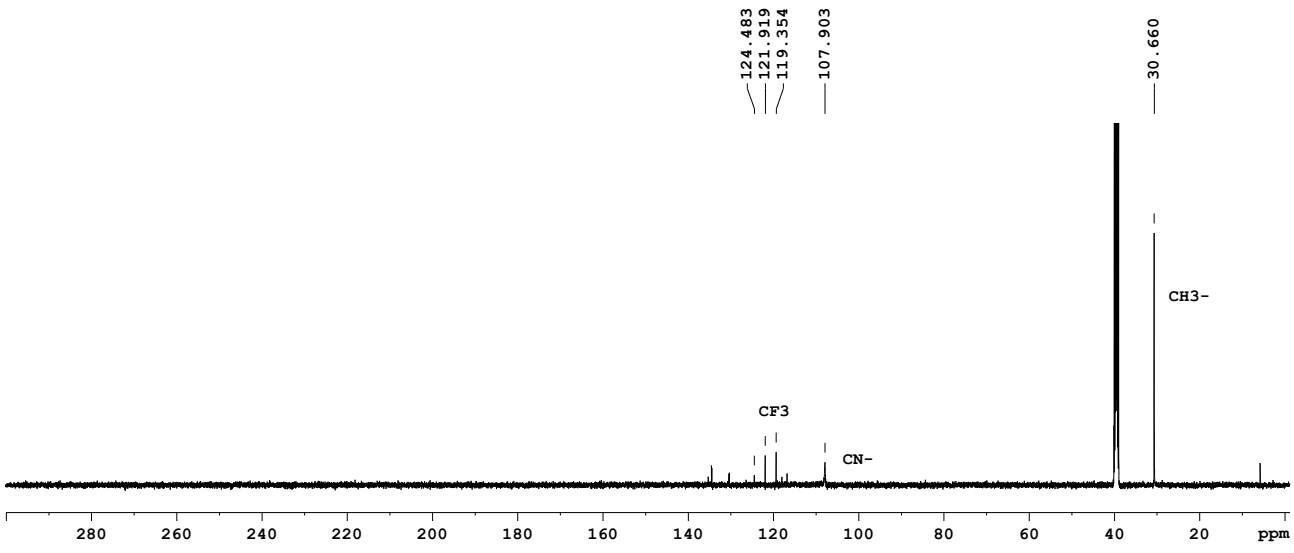

(c) $^{1}H,^{13}C$-HMBC (black) and $^{1}H,^{13}C$-HSQC (red) 2D spectra

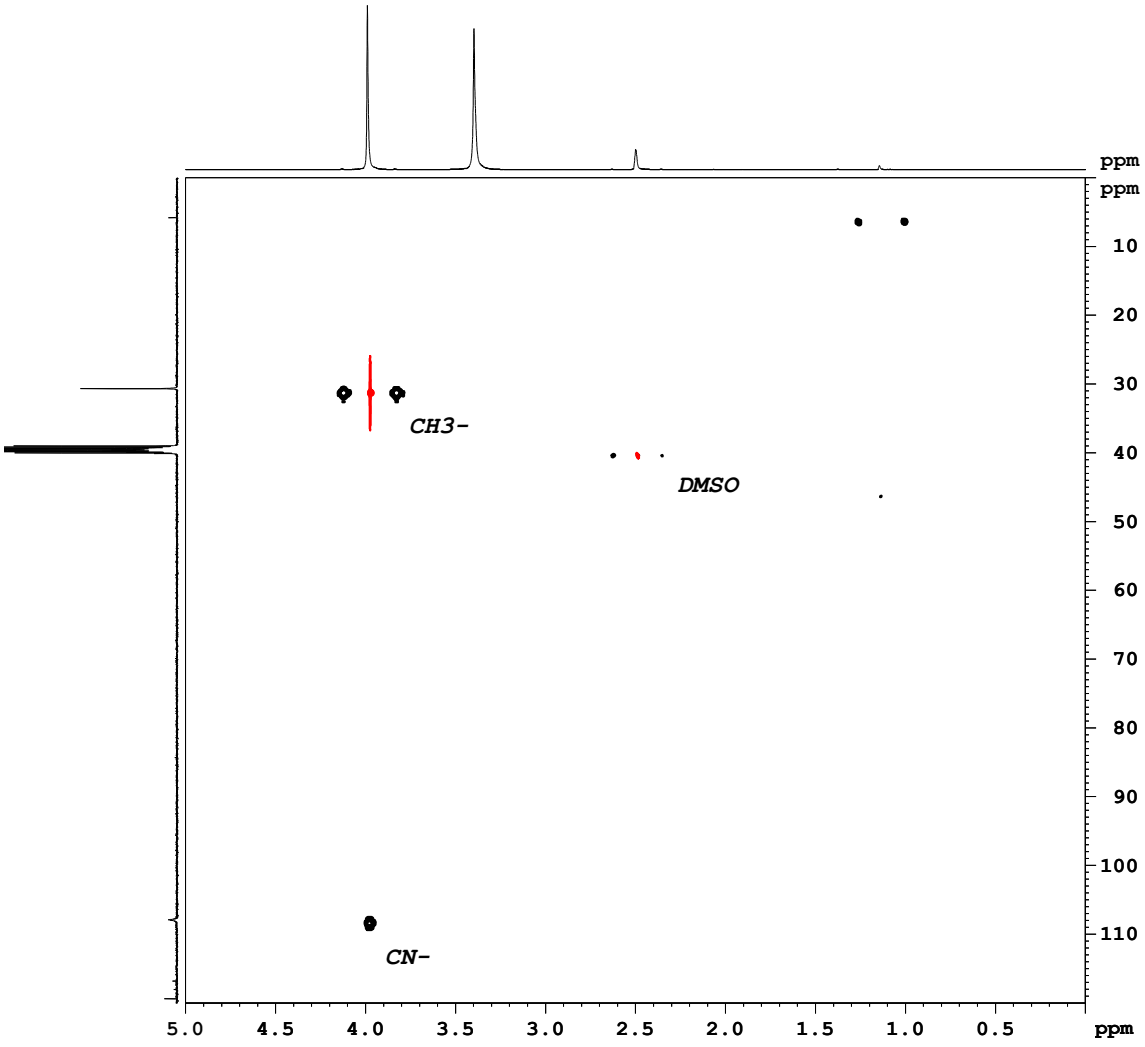

(d) ^{125}Te NMR

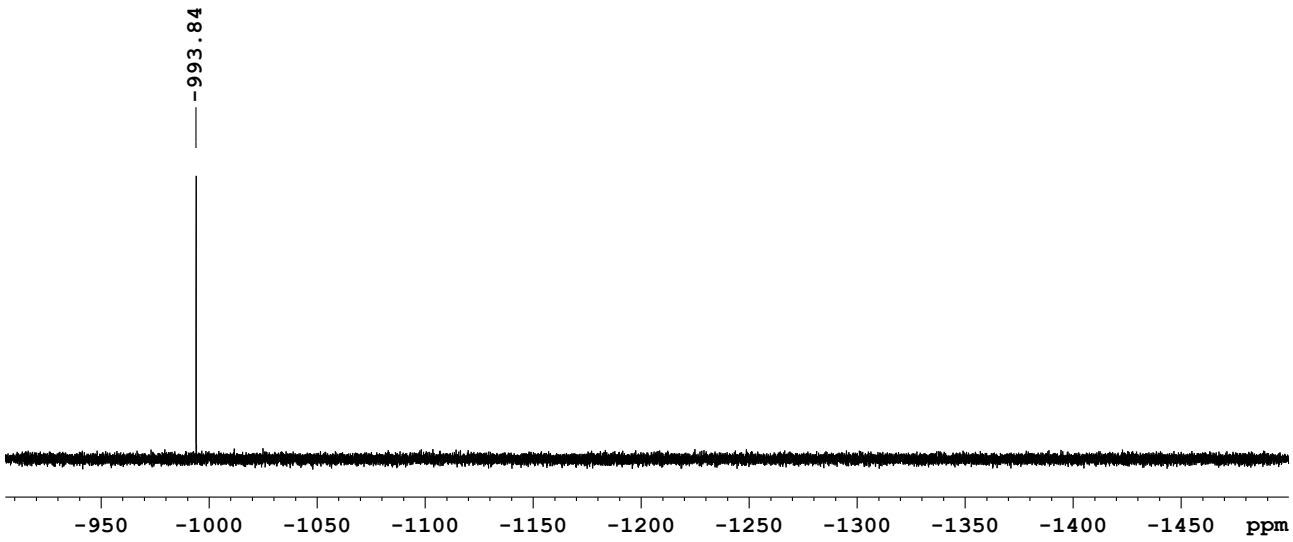

Figure S3. ^{1}H (a), ^{13}C (b), $^{1}H,^{13}C$-HMBC and $^{1}H,^{13}C$-HSQC (c) as well as ^{125}Te (d) NMR spectra of $[Re_6Te_8(CNCH_3)_6](CF_3SO_3)_2$.

(a) $\{[Re_6S_8(CH_3NC)_6](BF_4)\}^+$

Print of window 80: MS Spectrum

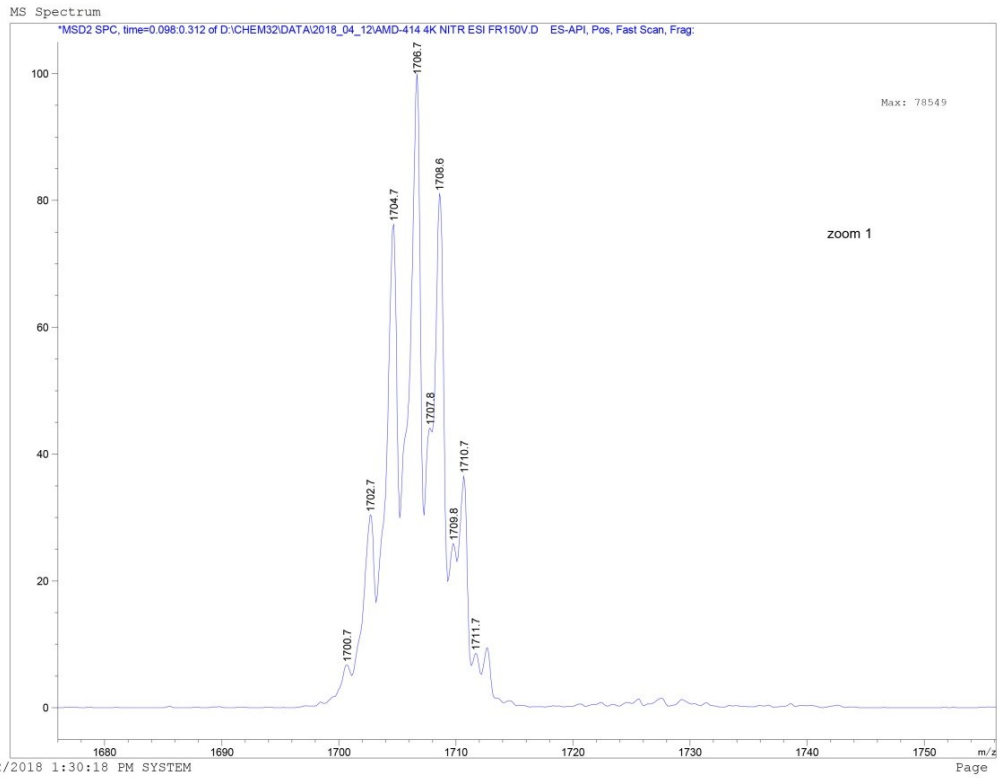

LCMS 4/12/2018 1:30:18 PM SYSTEM Page 1 of 1

(b) $\{[Re_6S_8(CH_3NC)_6](SO_3CF_3)\}^+$

Print of window 80: MS Spectrum

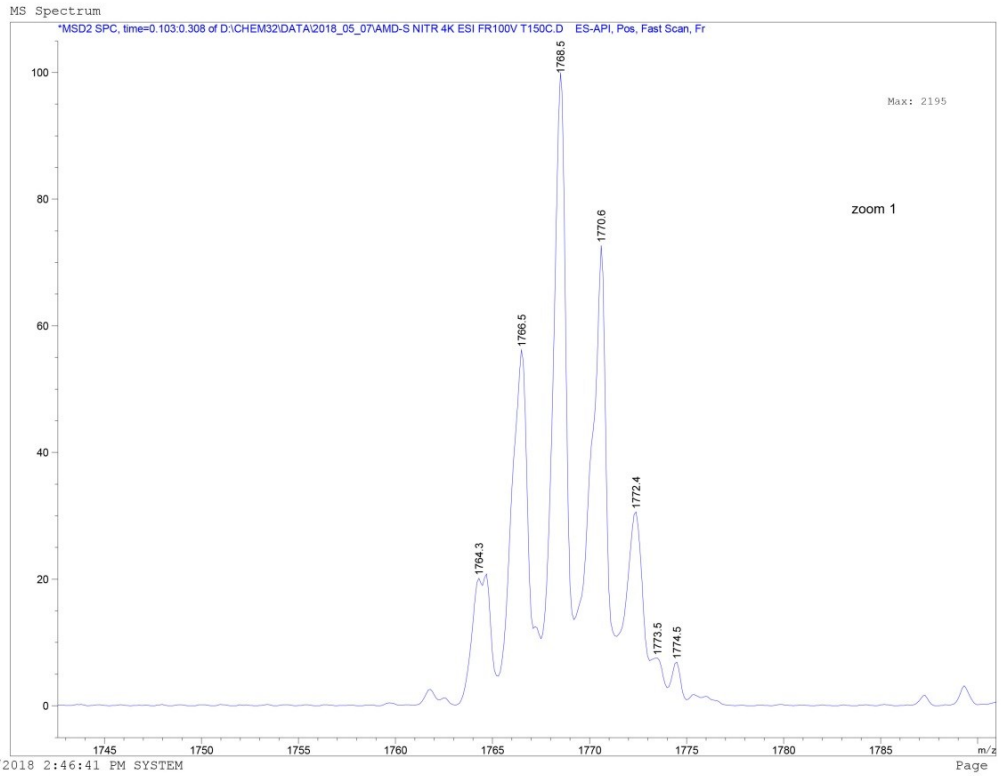

LCMS 5/7/2018 2:46:41 PM SYSTEM Page 1 of 1

(c) $\{[Re_6Se_8(CH_3NC)_6](BF_4)\}^+$

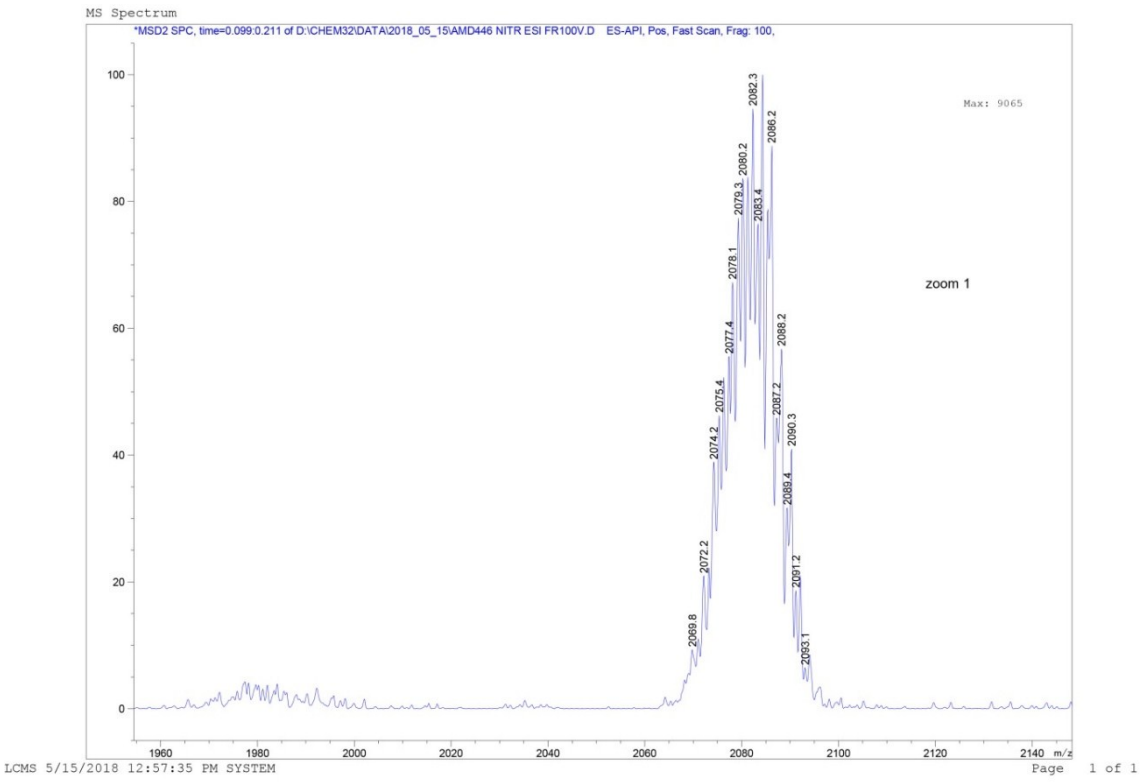

(d) $\{[Re_6Se_8(CH_3NC)_6](SO_3CF_3)\}^+$

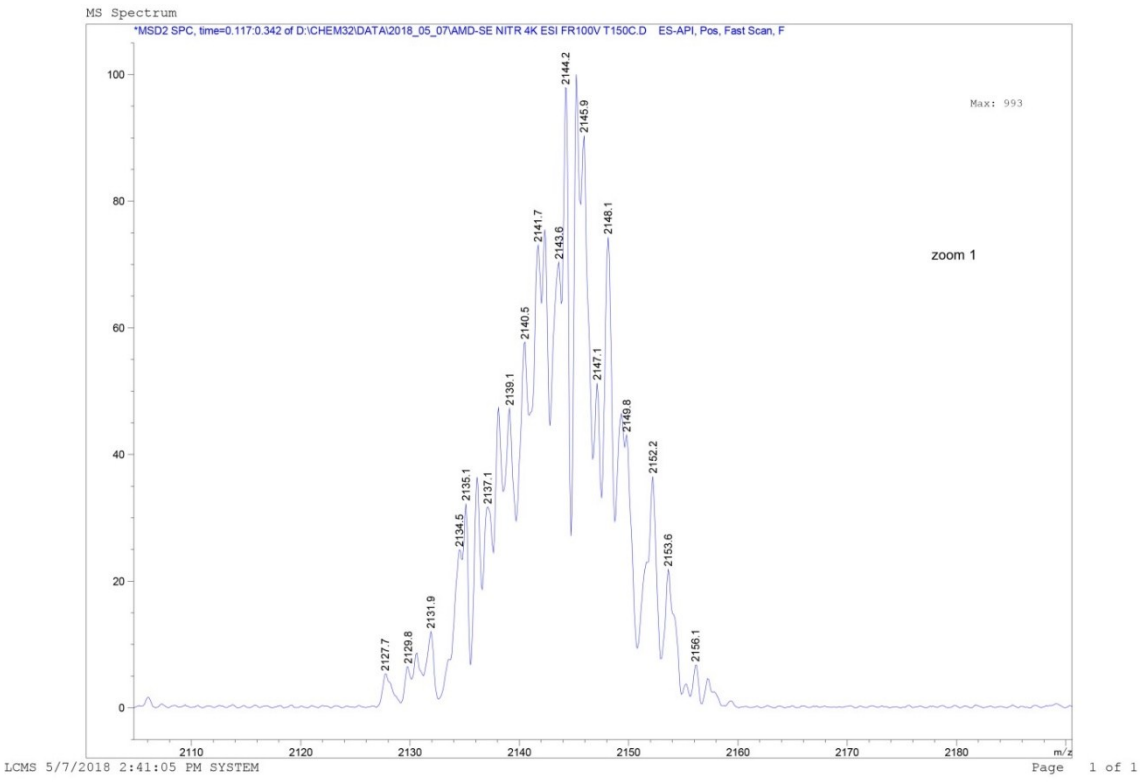

(e) $\{[Re_6Te_8(CH_3NC)_6](BF_4)\}^+$

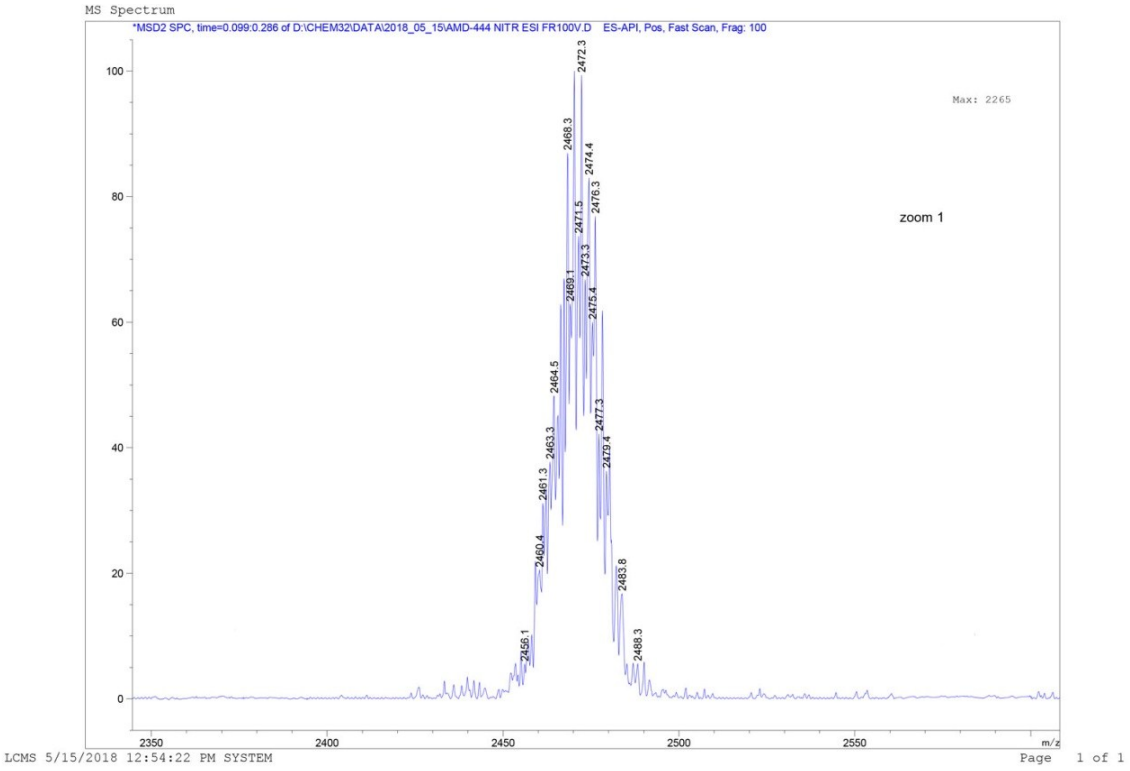

(f) $\{[Re_6Te_8(CH_3NC)_6](SO_3CF_3)\}^+$

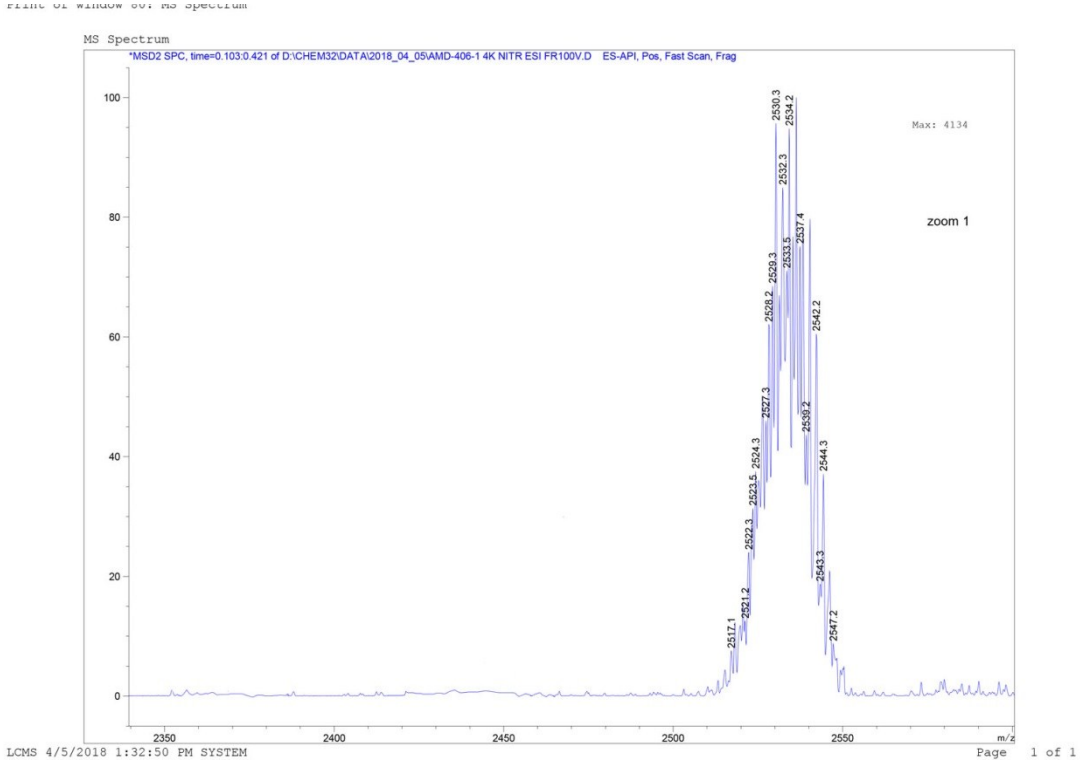

Figure S4. ESI-MS of the clusters **1** (a), **2** (b), **3** (c), **4** (d), **5** (e) and **6** (f).

(a)

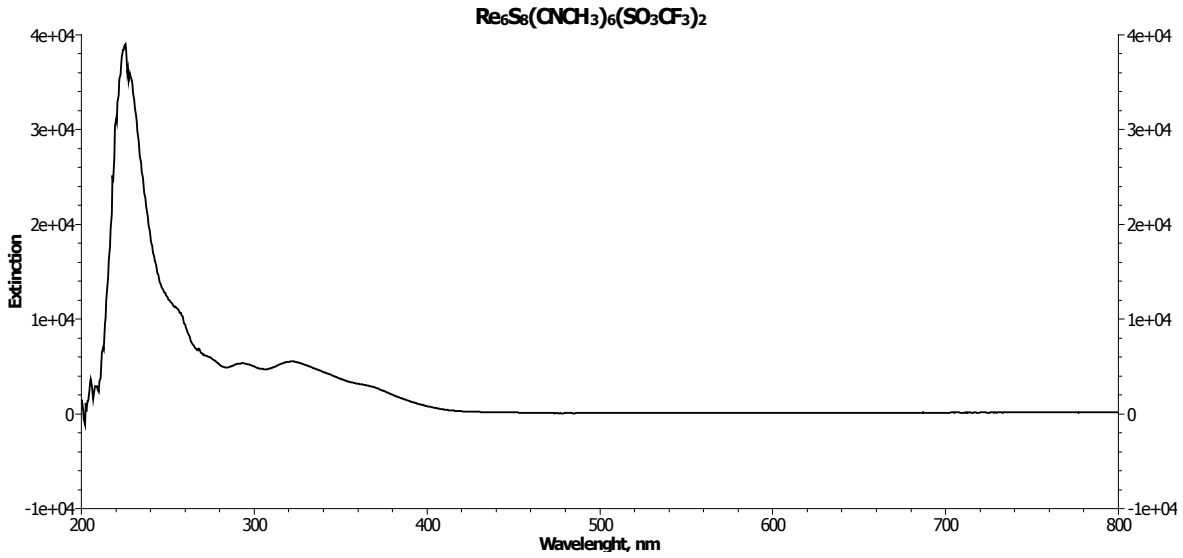

(b)

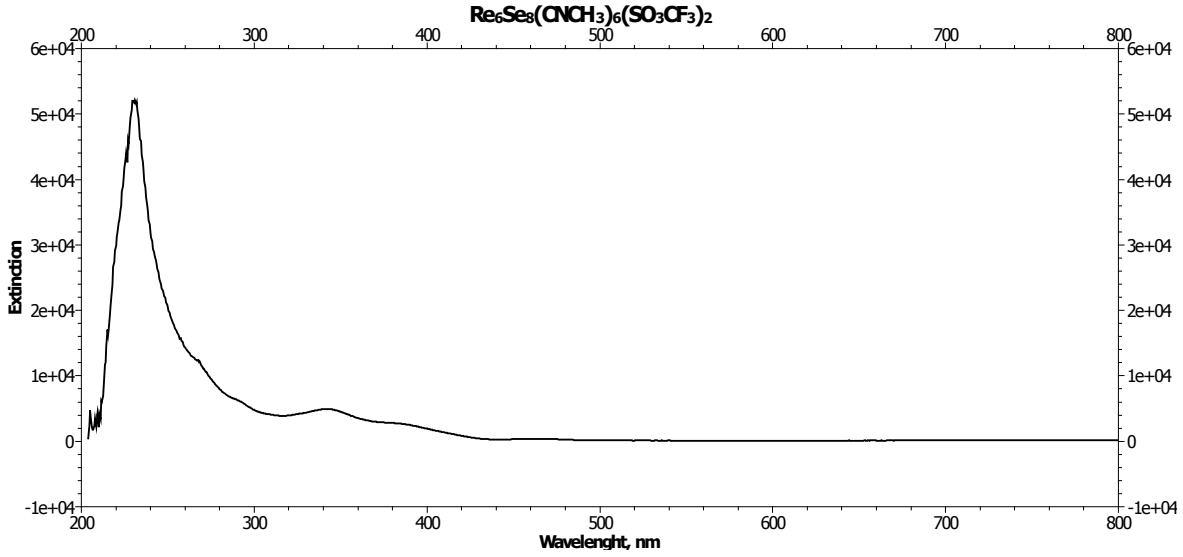

(c)

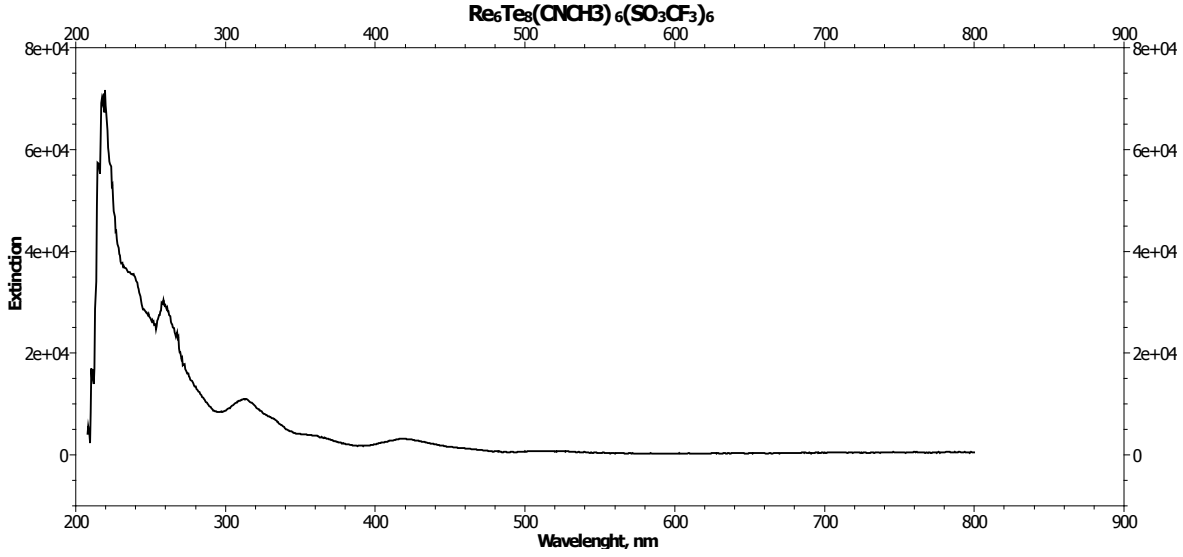

Fig. S5. UV-vis spectra of MeCN solutions of **2** (a), **4** (b) and **5** (c).

Table S1. Crystal Data and Structure Refinement for 2·CH_3CN, 3·$CH_3CN·H_2O$ and 5·3DMF

Parameter	**2**·CH_3CN	**3**·CH_3CN	**5**·3DMF
Empirical formula	$C_{18}H_{24}F_6N_8O_6Re_6S_{10}$	$C_{18}H_{29}B_2F_8N_9ORe_6Se_8$	$C_{21}H_{39}B_2F_8N_9O_3Re_6Te_8$
Formula weight	2000.25	2309.96	2777.23
Temperature/K	298	155.2	298
Crystal system	orthorhombic	monoclinic	monoclinic
Space group	*Pbcn*	$P2_1/c$	$P2_1/n$
a/Å	22.8829(13)	16.9966(11)	12.0153(4)
b/Å	11.7447(7)	23.4741(15)	24.6284(8)
c/Å	16.8444(9)	11.6818(6)	18.1398(5)
β/°	90	96.5236(13)	101.3530(10)
Volume/Å^3	4527.0(4)	4630.6(5)	5262.9(3)
Z	4	4	4
ρ_{calc} g/cm^3	2.935	3.306	3.505
μ/mm^{-1}	16.506	21.970	18.153
F(000)	3600	4028	4800
Crystal size/mm^3	0.35 × 0.13 × 0.08	0.41 × 0.10 × 0.06	0.15 × 0.10 × 0.03
2Θ range for data collection/°	3.56 to 50.052	2.412 to 50.484	2.824 to 51.436
Index ranges	–27 ≤ h ≤ 27, –13 ≤ k ≤ 13, –19 ≤ l ≤ 20	–20 ≤ h ≤ 20, –28 ≤ k ≤ 28, –8 ≤ l ≤ 14	–14 ≤ h ≤ 14, –27 ≤ k ≤ 30, –22 ≤ l ≤ 17
Reflections collected	48639	26281	48414
Independent reflections	3987 [R_{int} = 0.0568, R_{sigma} = 0.0281]	8783 [R_{int} = 0.0486, R_{sigma} = 0.0569]	10017 [R_{int} = 0.0532, R_{sigma} = 0.0466]
restraints/parameters	0/230	29/ 440	46/423
Goodness-of-fit on F^2	1.241	1.110	1.040
Final R indexes [I>=2σ (I)]	R_1 = 0.0678, wR_2 = 0.1559	R_1 = 0.0491, wR_2 = 0.1064	R_1 = 0.0379, wR_2 = 0.0782
Final R indexes [all data]	R_1 = 0.0837, wR_2 = 0.1653	R_1 = 0.0730, wR_2 = 0.1154	R_1 = 0.0644, wR_2 = 0.0888
Largest diff. peak/hole / e Å^{-3}	2.93/–2.30	2.35/ –2.50	1.38/–1.04

Table S2. Bond Lengths in the Structures 2·CH_3CN, 3·$CH_3CN·H_2O$ and 5·3DMF

5·3DMF				**3**·CH_3CN				**2**·CH_3CN	
Atoms	**Length/Å**	**Atoms**	**Length/Å**	**Atoms**	**Length/Å**	**Atoms**	**Length/Å**	**Atoms**	**Length/Å**
Re1 Re2	2.6792(6)	Re4 Re5^2	2.6872(6)	Re1 Re2^3	2.6328(7)	Re4 Re5^4	2.6308(8)	Re1 Re2^5	2.6084(12)
Re1 Re2^1	2.6856(6)	Re4 Re5	2.6924(7)	Re1 Re2	2.6352(8)	Re4 Re5	2.6364(9)	Re1 Re2	2.6024(13)
Re1 Re3^1	2.6859(6)	Re4 Re6^2	2.6973(6)	Re1 Re3	2.6294(8)	Re4 Re6	2.6311(9)	Re1 Re3	2.6023(12)
Re1 Re3	2.6895(6)	Re4 Re6	2.6870(7)	Re1 Re3^3	2.6370(8)	Re4 Re6^4	2.6347(8)	Re1 Re3^5	2.6008(12)
Re1 Te1	2.6902(10)	Re4 Te5	2.6927(10)	Re1 Se1^3	2.5150(15)	Re4 Se5^4	2.5238(16)	Re1 S1	2.410(6)
Re1 Te2	2.6956(9)	Re4 Te6	2.6955(9)	Re1 Se2	2.5255(15)	Re4 Se6	2.5199(17)	Re1 S2	2.406(6)
Re1 Te3	2.6892(9)	Re4 Te7	2.6884(9)	Re1 Se3	2.5213(15)	Re4 Se7	2.5250(17)	Re1 S3^5	2.423(6)
Re1 Te4^1	2.6886(10)	Re4 Te8^2	2.6907(10)	Re1 Se4	2.5215(15)	Re4 Se8	2.5155(16)	Re1 S4^5	2.433(6)
Re1 C11	2.075(12)	Re4 C41	2.094(13)	Re1 C1	2.134(16)	Re4 C4	2.080(16)	Re1 C11	2.08(2)
Re2 Re1^1	2.6856(6)	Re5 Re4^2	2.6872(6)	Re2 Re1^3	2.6328(7)	Re5 Re4^4	2.6308(8)	Re2 Re1^5	2.6084(12)
Re2 Re3^1	2.6909(7)	Re5 Re6	2.6881(7)	Re2 Re3	2.6268(8)	Re5 Re6	2.6306(9)	Re2 Re3	2.6015(13)
Re2 Re3	2.6888(6)	Re5 Re6^2	2.6849(7)	Re2 Re3^3	2.6324(8)	Re5 Re6^4	2.6355(9)	Re2 Re3^5	2.6016(13)
Re2 Te1	2.6885(9)	Re5 Te5	2.6871(9)	Re2 Se1	2.5155(15)	Re5 Se5	2.5285(17)	Re2 S1	2.425(6)
Re2 Te2	2.6918(9)	Re5 Te6	2.6903(10)	Re2 Se2^3	2.5204(15)	Re5 Se6^4	2.5191(17)	Re2 S2	2.426(6)
Re2 Te3^1	2.6870(9)	Re5 Te7^2	2.6886(9)	Re2 Se3	2.5249(15)	Re5 Se7	2.5232(17)	Re2 S3	2.415(6)
Re2 Te4	2.6800(9)	Re5 Te8	2.6917(10)	Re2 Se4	2.5159(15)	Re5 Se8	2.5233(16)	Re2 S4	2.416(6)
Re2 C21	2.051(13)	Re5 C51	2.039(14)	Re2 C2	2.083(14)	Re5 C5	2.090(15)	Re2 C21	2.13(3)
Re3 Re1^1	2.6859(6)	Re6 Re4^2	2.6973(6)	Re3 Re1^3	2.6370(8)	Re6 Re4^4	2.6347(8)	Re3 Re1^5	2.6008(12)
Re3 Re2^1	2.6908(7)	Re6 Re5^2	2.6848(7)	Re3 Re2^3	2.6324(8)	Re6 Re5^4	2.6355(9)	Re3 Re2^5	2.6016(13)

Re3	Te1	2.6857(9)	Re6	Te5	2.6924(9)	Re3	Se1	2.5202(16)	Re6	Se5	2.5217(17)	Re3	S1	2.420(6)
Re3	Te2[1]	2.6944(9)	Re6	Te6[2]	2.6925(9)	Re3	Se2	2.5244(16)	Re6	Se6	2.5206(17)	Re3	S2[5]	2.430(6)
Re3	Te3	2.6924(9)	Re6	Te7	2.6867(10)	Re3	Se3[3]	2.5262(14)	Re6	Se7[4]	2.5203(15)	Re3	S3	2.421(6)
Re3	Te4	2.6872(9)	Re6	Te8	2.6895(10)	Re3	Se4	2.5215(14)	Re6	Se8	2.5204(15)	Re3	S4[5]	2.428(6)
Re3	C31	2.062(13)	Re6	C61	2.061(14)	Re3	C3	2.098(16)	Re6	C6	2.10(2)	Re3	C31	2.14(3)
Te2	Re3[1]	2.6943(9)	Te6	Re6[2]	2.6925(9)	Se1	Re1[3]	2.5150(15)	Se5	Re4[4]	2.5239(16)	S2	Re3[5]	2.430(6)
Te3	Re2[1]	2.6869(9)	Te7	Re5[2]	2.6886(9)	Se2	Re2[3]	2.5204(15)	Se6	Re5[4]	2.5191(16)	S3	Re1[5]	2.423(6)
Te4	Re1[1]	2.6886(10)	Te8	Re4[2]	2.6907(10)	Se3	Re3[3]	2.5261(14)	Se7	Re6[4]	2.5203(15)	S4	Re1[5]	2.433(6)
N12	C11	1.124(14)	N42	C41	1.121(14)	N1	C1	1.089(18)	N4	C4	1.145(19)	N12	C11	1.19(3)
N12	C13	1.433(16)	N42	C48	1.446(16)	N1	C11	1.481(18)	N4	C41	1.437(19)	N12	C13	1.40(3)
N22	C21	1.152(16)	N52	C51	1.160(16)	N2	C2	1.138(18)	N5	C5	1.140(18)	N22	C21	1.09(3)
N22	C23	1.441(18)	N52	C58	1.429(18)	N2	C21	1.44(2)	N5	C51	1.420(19)	N22	C23	1.46(4)
N32	C31	1.147(14)	N62	C61	1.141(15)	N3	C3	1.137(19)	N6	C6	1.13(2)	N32	C31	1.07(3)
N32	C33	1.440(15)	N62	C68	1.422(18)	N3	C31	1.46(2)	N6	C61	1.44(2)	N32	C33	1.45(4)

[1]1–*x*, 1–*y*, 1–*z*; [2]1–*x*, 1–*y*, –*z*; [3]–*x*, 1–*y*, 2–*z*; [4]1–*x*, 1–*y*, 2–*z*; [5]1–*x*, 2–*y*, 1–*z*

Table S3. Bond Angles for 2·CH_3CN

Atoms			Angle/°
Re2	Re1	Re2[1]	90.00(4)
Re3[1]	Re1	Re2[1]	59.92(4)
Re3	Re1	Re2	59.98(4)
Re3	Re1	Re2[1]	59.91(3)
Re3[1]	Re1	Re2	60.00(3)
Re3[1]	Re1	Re3	89.83(4)
S1	Re1	Re2[1]	117.46(15)
S1	Re1	Re2	57.71(15)
S1	Re1	Re3	57.57(15)
S1	Re1	Re3[1]	117.67(15)
S1	Re1	S3[1]	173.8(2)
S1	Re1	S4[1]	90.0(2)
S2	Re1	Re2	57.77(14)
S2	Re1	Re2[1]	117.80(15)
S2	Re1	Re3[1]	57.90(14)
S2	Re1	Re3	117.72(14)
S2	Re1	S1	90.0(2)
S2	Re1	S3[1]	90.1(2)
S2	Re1	S4[1]	174.0(2)
S3[1]	Re1	Re2[1]	57.23(14)
S3[1]	Re1	Re2	117.45(15)
S3[1]	Re1	Re3	117.11(14)
S3[1]	Re1	Re3[1]	57.49(15)
S3[1]	Re1	S4[1]	89.3(2)
S4[1]	Re1	Re2	117.48(15)
S4[1]	Re1	Re2[1]	57.15(14)
S4[1]	Re1	Re3[1]	117.04(14)
S4[1]	Re1	Re3	57.55(14)
C11	Re1	Re2[1]	133.7(7)
C11	Re1	Re2	136.3(7)
C11	Re1	Re3	135.9(5)
C11	Re1	Re3[1]	134.2(6)
C11	Re1	S1	94.5(7)
C11	Re1	S2	93.0(6)
C11	Re1	S3[1]	91.7(7)
C11	Re1	S4[1]	93.0(6)
Re1	Re2	Re1[1]	90.00(4)
Re3	Re2	Re1[1]	59.90(3)

Re3[1]	Re2	Re1	59.97(3)
Re3[1]	Re2	Re1[1]	59.93(3)
Re3	Re2	Re1	60.01(4)
Re3	Re2	Re3[1]	89.83(4)
S1	Re2	Re1	57.17(15)
S1	Re2	Re1[1]	117.28(15)
S1	Re2	Re3	57.42(14)
S1	Re2	Re3[1]	117.10(15)
S1	Re2	S2	89.2(2)
S2	Re2	Re1[1]	117.57(14)
S2	Re2	Re1	57.06(14)
S2	Re2	Re3	117.04(15)
S2	Re2	Re3[1]	57.68(14)
S3	Re2	Re1	117.55(16)
S3	Re2	Re1[1]	57.52(14)
S3	Re2	Re3[1]	117.42(15)
S3	Re2	Re3	57.57(15)
S3	Re2	S1	90.0(2)
S3	Re2	S2	173.7(2)
S3	Re2	S4	89.8(2)
S4	Re2	Re1[1]	57.77(15)
S4	Re2	Re1	117.69(15)
S4	Re2	Re3	117.63(15)
S4	Re2	Re3[1]	57.74(15)
S4	Re2	S1	173.8(2)
S4	Re2	S2	90.3(2)
C21	Re2	Re1[1]	136.2(7)
C21	Re2	Re1	133.8(7)
C21	Re2	Re3	136.7(8)
C21	Re2	Re3[1]	133.4(8)
C21	Re2	S1	93.7(9)
C21	Re2	S2	91.3(7)
C21	Re2	S3	95.0(7)
C21	Re2	S4	92.5(9)
Re1[1]	Re3	Re1	90.17(4)
Re1[1]	Re3	Re2	60.18(4)
Re1[1]	Re3	Re2[1]	60.03(4)
Re2	Re3	Re1	60.01(4)
Re2[1]	Re3	Re1	60.16(3)
Re2	Re3	Re2[1]	90.17(4)
S1	Re3	Re1	57.23(14)
S1	Re3	Re1[1]	117.76(15)
S1	Re3	Re2	57.62(15)
S1	Re3	Re2[1]	117.37(14)
S1	Re3	S2[1]	173.7(2)
S1	Re3	S3	90.0(2)
S1	Re3	S4[1]	89.8(2)
S2[1]	Re3	Re1	117.63(14)
S2[1]	Re3	Re1[1]	57.03(14)
S2[1]	Re3	Re2	117.19(15)
S2[1]	Re3	Re2[1]	57.52(14)
S3	Re3	Re1[1]	57.56(15)
S3	Re3	Re1	117.34(15)
S3	Re3	Re2	57.35(14)
S3	Re3	Re2[1]	117.55(15)
S3	Re3	S2[1]	89.6(2)
S3	Re3	S4[1]	173.8(2)
S4[1]	Re3	Re1	57.72(15)

S4[1]	Re3	Re1[1]	117.30(15)
S4[1]	Re3	Re2[1]	57.29(15)
S4[1]	Re3	Re2	117.69(15)
S4[1]	Re3	S2[1]	89.9(2)
C31	Re3	Re1[1]	135.0(6)
C31	Re3	Re1	134.8(6)
C31	Re3	Re2[1]	134.4(8)
C31	Re3	Re2	135.4(8)
C31	Re3	S1	93.3(7)
C31	Re3	S2[1]	93.0(7)
C31	Re3	S3	93.5(8)
C31	Re3	S4[1]	92.7(8)
Re1	S1	Re2	65.12(15)
Re1	S1	Re3	65.20(15)
Re3	S1	Re2	64.95(15)
Re1	S2	Re2	65.17(15)
Re1	S2	Re3[1]	65.06(15)
Re2	S2	Re3[1]	64.80(15)
Re2	S3	Re1[1]	65.25(15)
Re2	S3	Re3	65.08(15)
Re3	S3	Re1[1]	64.94(15)
Re2	S4	Re1[1]	65.09(16)
Re2	S4	Re3[1]	64.96(15)
Re3[1]	S4	Re1[1]	64.74(16)
C11	N12	C13	176(3)
C21	N22	C23	178(3)
C31	N32	C33	172(3)
N12	C11	Re1	171(2)
N22	C21	Re2	179(3)
N32	C31	Re3	175(3)

[1]1–*x*, 2–*y*, 1–*z*

Table S4. Bond Angles for 3·CH_3CN

Atom			Angle/°	Atom			Angle/°
Re2[1]	Re1	Re2	89.84(2)	Re5[2]	Re4	Re5	90.00(2)
Re2	Re1	Re3[1]	59.91(2)	Re5[2]	Re4	Re6[2]	59.94(2)
Re2[1]	Re1	Re3[1]	59.80(2)	Re5[2]	Re4	Re6	60.11(2)
Re3	Re1	Re2[1]	60.03(2)	Re6	Re4	Re5	59.92(2)
Re3	Re1	Re2	59.86(2)	Re6[2]	Re4	Re5	60.00(2)
Re3	Re1	Re3[1]	89.81(2)	Re6	Re4	Re6[2]	89.97(3)
Se1[1]	Re1	Re2[1]	58.45(4)	Se5[2]	Re4	Re5	118.47(4)
Se1[1]	Re1	Re2	118.41(4)	Se5[2]	Re4	Re5[2]	58.71(4)
Se1[1]	Re1	Re3	118.47(4)	Se5[2]	Re4	Re6	118.81(4)
Se1[1]	Re1	Re3[1]	58.51(4)	Se5[2]	Re4	Re6[2]	58.48(4)
Se1[1]	Re1	Se2	89.80(5)	Se5[2]	Re4	Se7	89.65(6)
Se1[1]	Re1	Se3	89.90(5)	Se6	Re4	Re5[2]	58.51(4)
Se1[1]	Re1	Se4	176.21(5)	Se6	Re4	Re5	118.45(5)
Se2	Re1	Re2[1]	58.45(4)	Se6	Re4	Re6[2]	118.44(4)
Se2	Re1	Re2	118.45(4)	Se6	Re4	Re6	58.55(4)
Se2	Re1	Re3	58.60(4)	Se6	Re4	Se5[2]	90.18(6)
Se2	Re1	Re3[1]	118.24(4)	Se6	Re4	Se7	176.21(6)
Se3	Re1	Re2[1]	118.38(4)	Se7	Re4	Re5	58.49(4)
Se3	Re1	Re2	58.59(4)	Se7	Re4	Re5[2]	118.37(4)
Se3	Re1	Re3[1]	58.59(4)	Se7	Re4	Re6[2]	58.43(4)
Se3	Re1	Re3	118.44(4)	Se7	Re4	Re6	118.39(5)
Se3	Re1	Se2	176.24(5)	Se8	Re4	Re5	58.60(4)

Se3	Re1	Se4	89.74(5)	Se8	Re4	$Re5^{2}$	118.70(4)
Se4	Re1	$Re2^{1}$	118.59(4)	Se8	Re4	$Re6^{2}$	118.58(4)
Se4	Re1	Re2	58.35(4)	Se8	Re4	Re6	58.59(4)
Se4	Re1	Re3	58.57(4)	Se8	Re4	$Se5^{2}$	176.60(5)
Se4	Re1	$Re3^{1}$	118.25(4)	Se8	Re4	Se6	90.00(6)
Se4	Re1	Se2	90.31(5)	Se8	Re4	Se7	89.95(6)
C1	Re1	$Re2^{1}$	134.6(4)	C4	Re4	Re5	135.4(4)
C1	Re1	Re2	135.5(4)	C4	Re4	$Re5^{2}$	134.5(4)
C1	Re1	Re3	134.7(4)	C4	Re4	Re6	133.1(4)
C1	Re1	$Re3^{1}$	135.5(4)	C4	Re4	$Re6^{2}$	137.0(4)
C1	Re1	$Se1^{1}$	91.9(4)	C4	Re4	$Se5^{2}$	92.8(4)
C1	Re1	Se2	91.3(4)	C4	Re4	Se6	90.2(4)
C1	Re1	Se3	92.4(4)	C4	Re4	Se7	93.6(4)
C1	Re1	Se4	91.9(4)	C4	Re4	Se8	90.6(4)
$Re1^{1}$	Re2	Re1	90.16(2)	$Re4^{2}$	Re5	Re4	90.00(2)
$Re3^{1}$	Re2	$Re1^{1}$	59.92(2)	$Re4^{2}$	Re5	$Re6^{2}$	59.95(2)
Re3	Re2	Re1	59.96(2)	Re6	Re5	$Re4^{2}$	60.10(2)
$Re3^{1}$	Re2	Re1	60.08(2)	Re6	Re5	Re4	59.94(2)
Re3	Re2	$Re1^{1}$	60.18(2)	$Re6^{2}$	Re5	Re4	59.97(2)
Re3	Re2	$Re3^{1}$	89.96(2)	Re6	Re5	$Re6^{2}$	89.97(3)
Se1	Re2	Re1	118.59(4)	Se5	Re5	Re4	118.41(5)
Se1	Re2	$Re1^{1}$	58.43(4)	Se5	Re5	$Re4^{2}$	58.53(4)
Se1	Re2	Re3	58.65(4)	Se5	Re5	Re6	58.48(4)
Se1	Re2	$Re3^{1}$	118.34(4)	Se5	Re5	$Re6^{2}$	118.47(4)
Se1	Re2	$Se2^{1}$	89.91(5)	$Se6^{2}$	Re5	Re4	118.46(5)
Se1	Re2	Se3	176.32(5)	$Se6^{2}$	Re5	$Re4^{2}$	58.54(4)
Se1	Re2	Se4	90.20(5)	$Se6^{2}$	Re5	Re6	118.63(4)
$Se2^{1}$	Re2	Re1	118.69(4)	$Se6^{2}$	Re5	$Re6^{2}$	58.50(4)
$Se2^{1}$	Re2	$Re1^{1}$	58.64(4)	$Se6^{2}$	Re5	Se5	90.10(6)
$Se2^{1}$	Re2	$Re3^{1}$	58.62(4)	$Se6^{2}$	Re5	Se7	89.75(6)
$Se2^{1}$	Re2	Re3	118.81(4)	$Se6^{2}$	Re5	Se8	176.26(6)
$Se2^{1}$	Re2	Se3	89.91(5)	Se7	Re5	Re4	58.55(4)
Se3	Re2	$Re1^{1}$	118.52(4)	Se7	Re5	$Re4^{2}$	118.38(4)
Se3	Re2	Re1	58.45(4)	Se7	Re5	$Re6^{2}$	58.44(4)
Se3	Re2	Re3	118.40(4)	Se7	Re5	Re6	118.48(5)
Se3	Re2	$Re3^{1}$	58.61(4)	Se7	Re5	Se5	176.25(6)
Se4	Re2	Re1	58.56(4)	Se7	Re5	Se8	89.81(5)
Se4	Re2	$Re1^{1}$	118.85(4)	Se8	Re5	Re4	58.31(4)
Se4	Re2	Re3	58.67(4)	Se8	Re5	$Re4^{2}$	118.60(4)
Se4	Re2	$Re3^{1}$	118.63(4)	Se8	Re5	$Re6^{2}$	118.27(4)
Se4	Re2	$Se2^{1}$	176.77(5)	Se8	Re5	Re6	58.51(4)
Se4	Re2	Se3	89.78(5)	Se8	Re5	Se5	90.10(5)
C2	Re2	$Re1^{1}$	134.2(4)	C5	Re5	$Re4^{2}$	134.0(4)
C2	Re2	Re1	135.4(4)	C5	Re5	Re4	136.0(4)
C2	Re2	Re3	131.5(4)	C5	Re5	Re6	135.2(4)
C2	Re2	$Re3^{1}$	138.6(4)	C5	Re5	$Re6^{2}$	134.8(4)
C2	Re2	Se1	88.9(4)	C5	Re5	Se5	91.3(5)
C2	Re2	$Se2^{1}$	93.7(4)	C5	Re5	$Se6^{2}$	90.9(4)
C2	Re2	Se3	94.8(4)	C5	Re5	Se7	92.4(5)
C2	Re2	Se4	89.6(4)	C5	Re5	Se8	92.8(4)
Re1	Re3	$Re1^{1}$	90.19(2)	Re4	Re6	$Re4^{2}$	90.03(3)
Re1	Re3	$Re2^{1}$	60.05(2)	Re4	Re6	$Re5^{2}$	59.94(2)
$Re2^{1}$	Re3	$Re1^{1}$	60.01(2)	$Re4^{2}$	Re6	$Re5^{2}$	60.03(2)
Re2	Re3	$Re1^{1}$	60.02(2)	Re5	Re6	Re4	60.14(2)
Re2	Re3	Re1	60.18(2)	Re5	Re6	$Re4^{2}$	59.95(2)
Re2	Re3	$Re2^{1}$	90.04(2)	Re5	Re6	$Re5^{2}$	90.03(3)
Se1	Re3	$Re1^{1}$	58.32(4)	Se5	Re6	$Re4^{2}$	58.56(4)
Se1	Re3	Re1	118.63(4)	Se5	Re6	Re4	118.86(5)

Se1	Re3	Re2	58.47(4)	Se5	Re6	Re5^{2}	118.59(4)
Se1	Re3	Re2^{1}	118.32(4)	Se5	Re6	Re5	58.74(4)
Se1	Re3	Se2	176.35(5)	Se6	Re6	Re4^{2}	118.46(5)
Se1	Re3	Se3^{1}	89.68(5)	Se6	Re6	Re4	58.52(4)
Se1	Re3	Se4	89.96(5)	Se6	Re6	Re5^{2}	58.44(4)
Se2	Re3	Re1	58.64(4)	Se6	Re6	Re5	118.65(5)
Se2	Re3	Re1^{1}	118.48(4)	Se6	Re6	Se5	176.56(6)
Se2	Re3	Re2	118.81(4)	Se7^{2}	Re6	Re4^{2}	58.61(4)
Se2	Re3	Re2^{1}	58.47(4)	Se7^{2}	Re6	Re4	118.48(5)
Se2	Re3	Se3^{1}	89.80(5)	Se7^{2}	Re6	Re5	118.55(5)
Se3^{1}	Re3	Re1	118.60(4)	Se7^{2}	Re6	Re5^{2}	58.55(4)
Se3^{1}	Re3	Re1^{1}	58.42(4)	Se7^{2}	Re6	Se5	89.81(5)
Se3^{1}	Re3	Re2	118.43(4)	Se7^{2}	Re6	Se6	89.78(5)
Se3^{1}	Re3	Re2^{1}	58.57(4)	Se7^{2}	Re6	Se8	176.35(6)
Se4	Re3	Re1	58.57(4)	Se8	Re6	Re4^{2}	118.55(5)
Se4	Re3	Re1^{1}	118.48(4)	Se8	Re6	Re4	58.41(4)
Se4	Re3	Re2	58.47(4)	Se8	Re6	Re5^{2}	118.34(5)
Se4	Re3	Re2^{1}	118.60(4)	Se8	Re6	Re5	58.62(4)
Se4	Re3	Se2	90.34(5)	Se8	Re6	Se5	90.33(5)
Se4	Re3	Se3^{1}	176.36(5)	Se8	Re6	Se6	89.87(5)
C3	Re3	Re1^{1}	136.7(4)	C6	Re6	Re4	134.6(5)
C3	Re3	Re1	132.9(4)	C6	Re6	Re4^{2}	135.3(5)
C3	Re3	Re2^{1}	137.7(5)	C6	Re6	Re5^{2}	137.1(6)
C3	Re3	Re2	132.2(5)	C6	Re6	Re5	132.9(6)
C3	Re3	Se1	91.3(5)	C6	Re6	Se5	90.4(6)
C3	Re3	Se2	92.3(5)	C6	Re6	Se6	93.0(6)
C3	Re3	Se3^{1}	95.0(4)	C6	Re6	Se7^{2}	93.5(5)
C3	Re3	Se4	88.6(4)	C6	Re6	Se8	90.2(5)
Re1^{1}	Se1	Re2	63.12(4)	Re4^{2}	Se5	Re5	62.76(4)
Re1^{1}	Se1	Re3	63.16(4)	Re6	Se5	Re4^{2}	62.96(4)
Re2	Se1	Re3	62.88(4)	Re6	Se5	Re5	62.78(4)
Re2^{1}	Se2	Re1	62.90(4)	Re4	Se6	Re6	62.93(4)
Re2^{1}	Se2	Re3	62.91(4)	Re5^{2}	Se6	Re4	62.94(4)
Re3	Se2	Re1	62.76(4)	Re5^{2}	Se6	Re6	63.06(4)
Re1	Se3	Re2	62.96(4)	Re5	Se7	Re4	62.97(4)
Re1	Se3	Re3^{1}	62.99(4)	Re6^{2}	Se7	Re4	62.96(4)
Re2	Se3	Re3^{1}	62.82(4)	Re6^{2}	Se7	Re5	63.01(4)
Re1	Se4	Re3	62.85(4)	Re4	Se8	Re5	63.10(4)
Re2	Se4	Re1	63.09(4)	Re4	Se8	Re6	63.00(4)
Re2	Se4	Re3	62.86(4)	Re6	Se8	Re5	62.87(4)
C1	N1	C11	177.5(17)	C4	N4	C41	178.3(18)
C2	N2	C21	175.9(16)	C5	N5	C51	179.6(18)
C3	N3	C31	177(2)	C6	N6	C61	175(2)
N1	C1	Re1	177.7(14)	N4	C4	Re4	177.5(14)
N2	C2	Re2	176.4(14)	N5	C5	Re5	178.3(15)
N3	C3	Re3	175.8(17)	N6	C6	Re6	178(2)

^{1}–*x*, 1–*y*, 2–*z*; ^{2}1–*x*, 1–*y*, 2–*z*

Table S5. Bond Angles for 5·3DMF

Atoms			Angle/°	Atoms			Angle/°
Re2	Re1	Re2^{1}	90.091(19)	Re5^{2}	Re4	Re5	89.755(19)
Re2	Re1	Re3	60.109(16)	Re5	Re4	Re6^{2}	59.755(17)
Re2^{1}	Re1	Re3	60.080(17)	Re5^{2}	Re4	Re6^{2}	59.897(17)
Re2^{1}	Re1	Re3^{1}	60.077(16)	Re5^{2}	Re4	Te5	120.00(3)
Re2	Re1	Re3^{1}	60.205(17)	Re5	Re4	Te5	59.87(2)
Re2^{1}	Re1	Te1	119.98(3)	Re5	Re4	Te6	59.91(2)

Re2	Re1	Te1	60.09(2)	Re5^{2}	Re4	Te6	119.80(3)
Re2^{1}	Re1	Te2	120.17(3)	Re5^{2}	Re4	Te7	60.02(2)
Re2	Re1	Te2	60.11(2)	Re5^{2}	Re4	Te8^{2}	60.07(2)
Re2^{1}	Re1	Te3	59.99(2)	Re6	Re4	Re5	59.959(17)
Re2	Re1	Te3	120.18(2)	Re6	Re4	Re5^{2}	59.944(17)
Re2	Re1	Te4^{1}	120.20(3)	Re6	Re4	Re6^{2}	89.86(2)
Re2^{1}	Re1	Te4^{1}	59.83(2)	Re6	Re4	Te5	60.06(2)
Re3^{1}	Re1	Re3	90.316(18)	Re6	Re4	Te6	119.87(3)
Re3	Re1	Te1	59.90(2)	Re6	Re4	Te7	59.98(2)
Re3^{1}	Re1	Te1	120.30(3)	Re6	Re4	Te8^{2}	120.01(3)
Re3^{1}	Re1	Te2	60.09(2)	Te5	Re4	Re6^{2}	119.62(3)
Re3	Re1	Te2	120.22(3)	Te5	Re4	Te6	89.73(3)
Re3^{1}	Re1	Te3	120.06(3)	Te6	Re4	Re6^{2}	59.90(2)
Re3^{1}	Re1	Te4^{1}	60.00(2)	Te7	Re4	Re5	119.93(3)
Te1	Re1	Te2	90.14(3)	Te7	Re4	Re6^{2}	119.92(3)
Te3	Re1	Re3	60.07(2)	Te7	Re4	Te5	90.29(3)
Te3	Re1	Te1	89.98(3)	Te7	Re4	Te6	179.79(4)
Te3	Re1	Te2	179.70(3)	Te7	Re4	Te8^{2}	90.20(3)
Te4^{1}	Re1	Re3	119.90(3)	Te8^{2}	Re4	Re5	119.64(3)
Te4^{1}	Re1	Te1	179.57(3)	Te8^{2}	Re4	Re6^{2}	59.89(2)
Te4^{1}	Re1	Te2	90.29(3)	Te8^{2}	Re4	Te5	179.45(3)
Te4^{1}	Re1	Te3	89.60(3)	Te8^{2}	Re4	Te6	89.78(3)
C11	Re1	Re2^{1}	135.4(3)	C41	Re4	Re5^{2}	132.6(3)
C11	Re1	Re2	134.5(3)	C41	Re4	Re5	137.7(3)
C11	Re1	Re3^{1}	134.5(3)	C41	Re4	Re6^{2}	136.0(4)
C11	Re1	Re3	135.1(3)	C41	Re4	Re6	134.0(4)
C11	Re1	Te1	89.9(3)	C41	Re4	Te5	91.3(4)
C11	Re1	Te2	89.4(3)	C41	Re4	Te6	92.6(3)
C11	Re1	Te3	90.4(3)	C41	Re4	Te7	87.6(3)
C11	Re1	Te4^{1}	90.1(3)	C41	Re4	Te8^{2}	89.0(4)
Re1	Re2	Re1^{1}	89.908(18)	Re4^{2}	Re5	Re4	90.244(19)
Re1	Re2	Re3^{1}	60.019(17)	Re4^{2}	Re5	Re6	60.239(16)
Re1^{1}	Re2	Re3	59.968(16)	Re4^{2}	Re5	Te6	120.15(3)
Re1	Re2	Re3	60.135(16)	Re4^{2}	Re5	Te7^{2}	60.01(2)
Re1^{1}	Re2	Re3^{1}	60.032(16)	Re4^{2}	Re5	Te8	60.03(2)
Re1^{1}	Re2	Te1	119.89(2)	Re6	Re5	Re4	59.921(17)
Re1	Re2	Te1	60.16(2)	Re6^{2}	Re5	Re4^{2}	60.026(17)
Re1^{1}	Re2	Te2	120.11(3)	Re6^{2}	Re5	Re4	60.213(17)
Re1	Re2	Te2	60.25(2)	Re6^{2}	Re5	Re6	90.10(2)
Re1	Re2	Te3^{1}	120.10(3)	Re6^{2}	Re5	Te5	120.28(3)
Re1^{1}	Re2	Te3^{1}	60.07(2)	Re6	Re5	Te6	120.02(3)
Re1	Re2	Te4	120.20(2)	Re6^{2}	Re5	Te6	60.12(2)
Re3	Re2	Re3^{1}	90.224(19)	Re6	Re5	Te7^{2}	120.25(3)
Re3^{1}	Re2	Te2	60.07(2)	Re6^{2}	Re5	Te7^{2}	60.00(2)
Re3	Re2	Te2	120.38(3)	Re6^{2}	Re5	Te8	120.06(3)
Te1	Re2	Re3	59.93(2)	Re6	Re5	Te8	59.99(2)
Te1	Re2	Re3^{1}	120.17(3)	Te5	Re5	Re4	60.07(2)
Te1	Re2	Te2	90.26(3)	Te5	Re5	Re4^{2}	120.36(3)
Te3^{1}	Re2	Re3^{1}	60.09(2)	Te5	Re5	Re6	60.12(2)
Te3^{1}	Re2	Re3	120.04(3)	Te5	Re5	Te6	89.96(3)
Te3^{1}	Re2	Te1	179.71(3)	Te5	Re5	Te7^{2}	179.59(3)
Te3^{1}	Re2	Te2	90.00(3)	Te5	Re5	Te8	89.90(3)
Te4	Re2	Re1^{1}	60.14(2)	Te6	Re5	Re4	60.10(2)
Te4	Re2	Re3^{1}	120.17(3)	Te6	Re5	Te8	179.82(3)
Te4	Re2	Re3	60.07(2)	Te7^{2}	Re5	Re4	120.21(3)
Te4	Re2	Te1	89.92(3)	Te7^{2}	Re5	Te6	89.97(3)
Te4	Re2	Te2	179.54(3)	Te7^{2}	Re5	Te8	90.17(3)
Te4	Re2	Te3^{1}	89.83(3)	Te8	Re5	Re4	119.91(3)

C21	Re2	Re1[1]	134.4(4)	C51	Re5	Re4	135.3(4)
C21	Re2	Re1	135.7(4)	C51	Re5	Re4[2]	134.4(4)
C21	Re2	Re3[1]	136.0(4)	C51	Re5	Re6	136.2(4)
C21	Re2	Re3	133.8(3)	C51	Re5	Re6[2]	133.7(4)
C21	Re2	Te1	89.6(4)	C51	Re5	Te5	90.9(4)
C21	Re2	Te2	91.0(3)	C51	Re5	Te6	89.3(4)
C21	Re2	Te3[1]	90.2(4)	C51	Re5	Te7[2]	88.7(4)
C21	Re2	Te4	88.6(3)	C51	Re5	Te8	90.6(4)
Re1[1]	Re3	Re1	89.683(18)	Re4	Re6	Re4[2]	90.14(2)
Re1[1]	Re3	Re2	59.956(16)	Re4	Re6	Re5	60.120(17)
Re1[1]	Re3	Re2[1]	59.776(17)	Re4	Re6	Te5	60.07(2)
Re1	Re3	Re2[1]	59.887(16)	Re4	Re6	Te6[2]	120.07(3)
Re1	Re3	Te2[1]	119.87(3)	Re4	Re6	Te8	120.19(3)
Re1[1]	Re3	Te2[1]	60.14(2)	Re5[2]	Re6	Re4	60.031(17)
Re1[1]	Re3	Te3	119.66(3)	Re5	Re6	Re4[2]	59.865(17)
Re1	Re3	Te3	59.96(2)	Re5[2]	Re6	Re4[2]	60.031(17)
Re1[1]	Re3	Te4	60.05(2)	Re5[2]	Re6	Re5	89.90(2)
Re2	Re3	Re1	59.756(16)	Re5	Re6	Te5	59.92(2)
Re2	Re3	Re2[1]	89.776(19)	Re5[2]	Re6	Te5	120.10(3)
Re2[1]	Re3	Te2[1]	59.98(2)	Re5	Re6	Te6[2]	119.88(3)
Re2	Re3	Te2[1]	120.09(3)	Re5[2]	Re6	Te6[2]	60.04(2)
Re2[1]	Re3	Te3	59.89(2)	Re5[2]	Re6	Te7	60.07(2)
Re2	Re3	Te3	119.71(2)	Re5[2]	Re6	Te8	119.96(3)
Te1	Re3	Re1	60.06(2)	Re5	Re6	Te8	60.07(2)
Te1	Re3	Re1[1]	119.99(3)	Te5	Re6	Re4[2]	119.79(3)
Te1	Re3	Re2	60.03(2)	Te5	Re6	Te6[2]	179.70(4)
Te1	Re3	Re2[1]	119.95(3)	Te6[2]	Re6	Re4[2]	60.01(2)
Te1	Re3	Te2[1]	179.83(4)	Te7	Re6	Re4	60.04(2)
Te1	Re3	Te3	90.00(3)	Te7	Re6	Re4[2]	120.10(3)
Te1	Re3	Te4	89.83(3)	Te7	Re6	Re5	120.16(3)
Te3	Re3	Te2[1]	89.83(3)	Te7	Re6	Te5	90.33(3)
Te4	Re3	Re1	119.56(2)	Te7	Re6	Te6[2]	89.96(3)
Te4	Re3	Re2	59.80(2)	Te7	Re6	Te8	179.77(4)
Te4	Re3	Re2[1]	119.82(3)	Te8	Re6	Re4[2]	59.93(2)
Te4	Re3	Te2[1]	90.34(3)	Te8	Re6	Te5	89.84(3)
Te4	Re3	Te3	179.50(3)	Te8	Re6	Te6[2]	89.87(3)
C31	Re3	Re1[1]	135.3(3)	C61	Re6	Re4[2]	136.2(4)
C31	Re3	Re1	134.9(3)	C61	Re6	Re4	133.6(4)
C31	Re3	Re2[1]	137.2(3)	C61	Re6	Re5	135.0(4)
C31	Re3	Re2	133.0(3)	C61	Re6	Re5[2]	135.0(4)
C31	Re3	Te1	88.4(3)	C61	Re6	Te5	89.1(3)
C31	Re3	Te2[1]	91.6(3)	C61	Re6	Te6[2]	90.9(3)
C31	Re3	Te3	91.6(3)	C61	Re6	Te7	89.0(4)
C31	Re3	Te4	88.9(3)	C61	Re6	Te8	90.8(4)
Re2	Te1	Re1	59.75(2)	Re5	Te5	Re4	60.06(2)
Re3	Te1	Re1	60.04(2)	Re5	Te5	Re6	59.96(2)
Re3	Te1	Re2	60.04(2)	Re6	Te5	Re4	59.87(2)
Re2	Te2	Re1	59.65(2)	Re5	Te6	Re4	59.99(2)
Re2	Te2	Re3[1]	59.95(2)	Re5	Te6	Re6[2]	59.84(2)
Re3[1]	Te2	Re1	59.78(2)	Re6[2]	Te6	Re4	60.08(2)
Re1	Te3	Re3	59.97(2)	Re4	Te7	Re5[2]	59.97(2)
Re2[1]	Te3	Re1	59.94(2)	Re6	Te7	Re4	59.99(2)
Re2[1]	Te3	Re3	60.03(2)	Re6	Te7	Re5[2]	59.93(2)
Re2	Te4	Re1[1]	60.03(2)	Re4[2]	Te8	Re5	59.90(2)
Re2	Te4	Re3	60.13(2)	Re6	Te8	Re4[2]	60.18(2)
Re3	Te4	Re1[1]	59.95(2)	Re6	Te8	Re5	59.94(2)
C11	N12	C13	176.1(16)	C41	N42	C43	177.2(14)
C21	N22	C23	176.8(16)	C51	N52	C53	177.8(16)

C31	N32	C33	178.7(13)	C61	N62	C63	178.0(17)
N12	C11	Re1	178.0(12)	N42	C41	Re4	176.8(11)
N22	C21	Re2	178.0(12)	N52	C51	Re5	177.4(12)
N32	C31	Re3	179.0(12)	N62	C61	Re6	176.9(13)

[1]1–*x*, 1–*y*, 1–*z*; [2]1–*x*, 1–*y*, –*z*

(a)

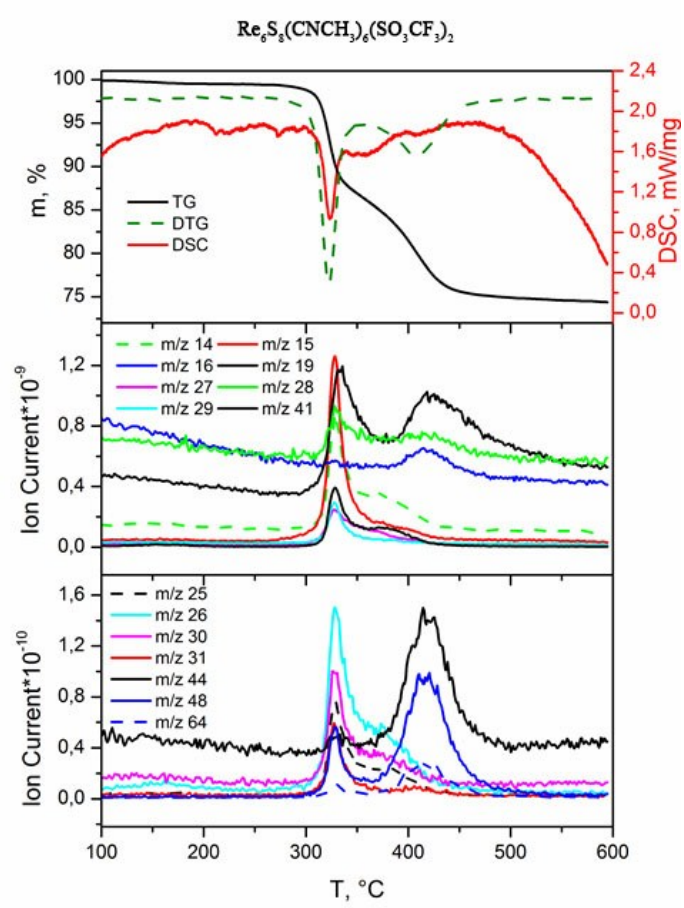
Re6S8(CNCH3)6(SO3CF3)2
m, %
DSC, mW/mg
TG
DTG
DSC
Ion Current*10-9
m/z 14
m/z 15
m/z 16
m/z 19
m/z 27
m/z 28
m/z 29
m/z 41
Ion Current*10-10
m/z 25
m/z 26
m/z 30
m/z 31
m/z 44
m/z 48
m/z 64
T, °C

(b)

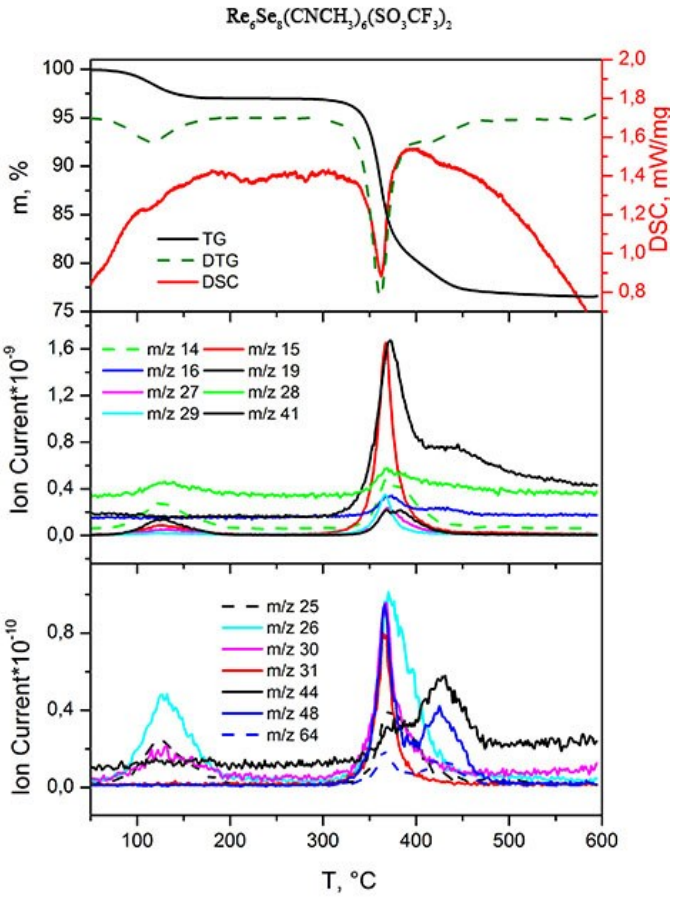
Re6Se8(CNCH3)6(SO3CF3)2
m, %
DSC, mW/mg
TG
DTG
DSC
Ion Current*10-9
m/z 14
m/z 15
m/z 16
m/z 19
m/z 27
m/z 28
m/z 29
m/z 41
Ion Current*10-10
m/z 25
m/z 26
m/z 30
m/z 31
m/z 44
m/z 48
m/z 64
T, °C

(c)

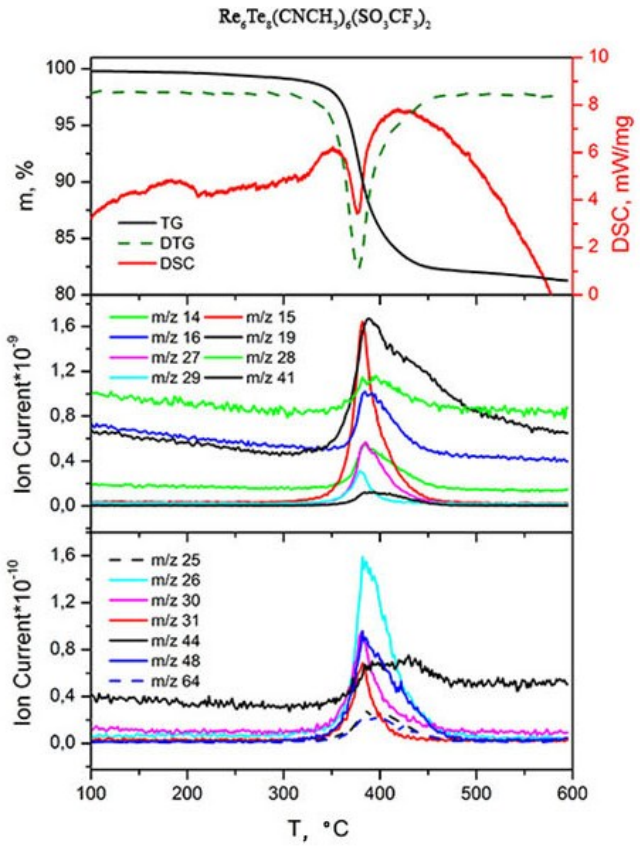

Figure S6. Thermal analysis data for **2** (a), **4** (b) and **6** (c).

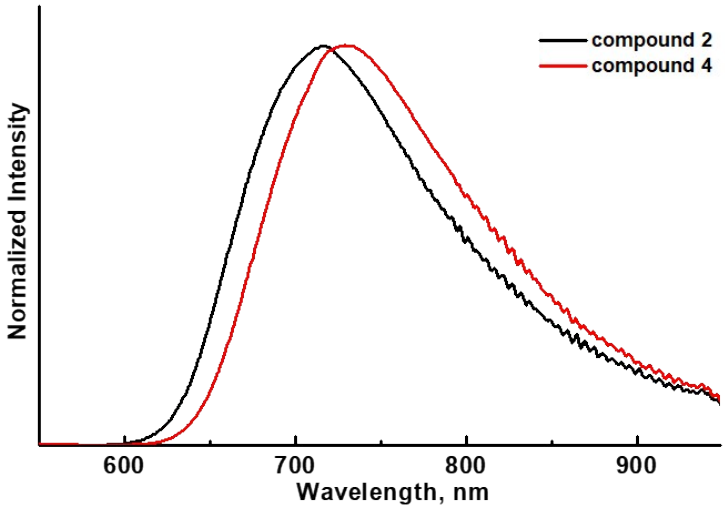

Figure S7. Normalized photoemission spectra of the powdered samples of **2** and **4**.

The spectra of X-ray induced luminescence were recorded from neat powders of **2**, **4**, and **6** at ambient conditions on a home-built MARY spectrometer described elsewhere[1] following the protocol developed specifically for powdered samples of cluster complexes.[2] Experimental details are given in the SI. The spectrometer has, among other operation modes, provisions to detect spectrally resolved optical emission from samples exposed to X-rays, which we took advantage of in this work. The samples were prepared as "islets" with dimensions of 3x8 mm and thickness of about 0.1 mm, ground in a mortar and applied through a stencil onto an aluminum plate covered with polypropylene-based double-sided Scotch tape. The reasons for using such thin naked samples, and the procedures of sample preparation and spectral processing have been discussed at length in a previous publication.[2] The sample was mounted vertically at 45 degrees to both the incident X-ray beam and the detection system, which were horizontal and normal to each other, and was directly exposed to the incident X-ray beam and to the optics of the light-collecting portion of the detection system. X-rays were generated by a CW X-ray tube (BSV-27-Mo, Svetlana, St. Petersburg, Russia, 40 kV x 20 mA). For excitation the entire sample strip was exposed to unfiltered bremsstrahlung. The detection channel comprised a quartz optical imaging system, a grating monochromator (MDR-206, LOMO Photonics, St. Petersburg, Russia, objective focus length 180 mm, grating 1200 lines per mm, inverse linear dispersion 4.3 nm mm^{-1}) with slits set to 2.2 mm/2.2 mm (spectral resolution about 10 nm), and a Hamamatsu H10493-012 photosensor module. The X-ray induced luminescence spectra were corrected for spectral sensitivity and baseline of the detector, and normalized by the number of moles of the compound. Each spectrum contains 512 wavelength points, and is the average of 36 independent wavelength scans of 18 minutes each. At the red end of the spectral range the spectra were cut off at an arbitrarily chosen limit of 835 nm, beyond which the sensitivity of the detector was too low for reliable results. Nevertheless, the available spectral range is sufficient to cover the maxima of the emission bands for all the complexes studied in this work. Although the absolute intensities of X-ray induced luminescence spectra cannot be interpreted from first principles due to lack of a meaningful measure of excitation efficiency, a series of spectra recorded in nominally identical conditions can be compared to each other for relative efficiencies of X-ray-induced emissions given by area under the spectral line, which is the closest counterpart to standard photoluminescence quantum yield, common in optical studies.

1. Kalneus, E. V.; Melnikov, A. R.; Korolev, V. V.; Ivannikov, V. I.; Stass, D. V. A low-field magnetically affected reaction yield (MARY) spectrometer with spectral fluorescence resolution. *Appl. Magn. Reson.* **2013**, *44*, 81-96.

2. Evtushok, D. V.; Melnikov, A. R.; Vorotnikova, N. A.; Vorotnikov, Y. A.; Ryadun, A. A.; Kuratieva, N. V.; Kozyr, K. V.; Obedinskaya, N. R.; Kretov, E. I.; Novozhilov, I. N.; Mironov, Y. V.; Stass, D. V.; Efremova, O. A.; Shestopalov, M. A. A comparative study of optical properties and X-ray induced luminescence of octahedral molybdenum and tungsten cluster complexes. *Dalton Trans.* **2017**, *46*, 11738-11747.

(a) X-ray-induced luminescence of **2**

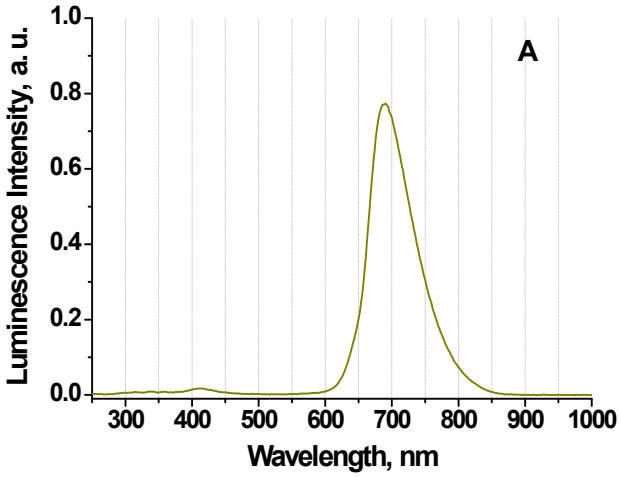

Uncorrected spectrum

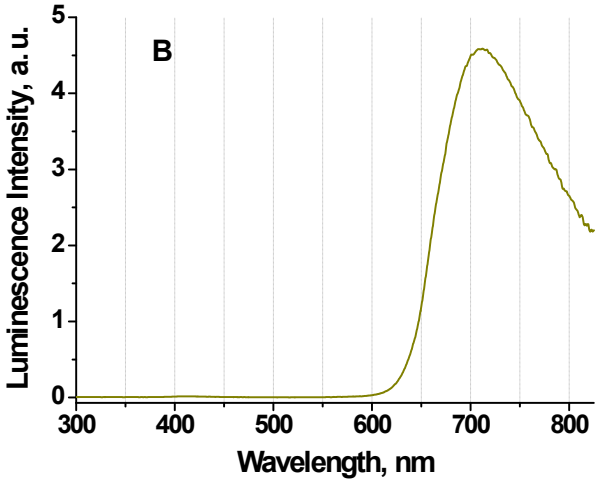

Corrected spectrum

(b) X-ray-induced luminescence of **4**

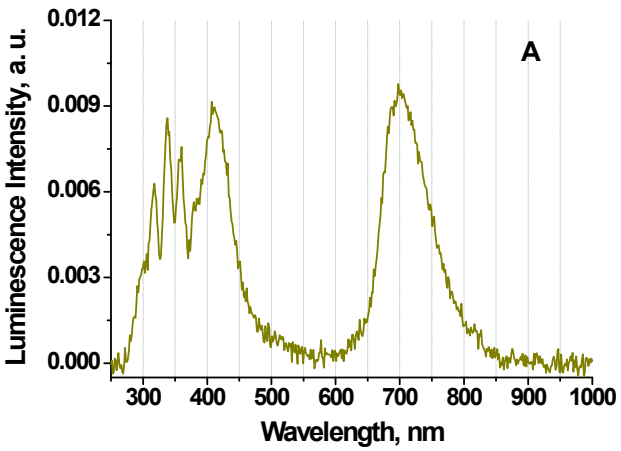

Uncorrected spectrum

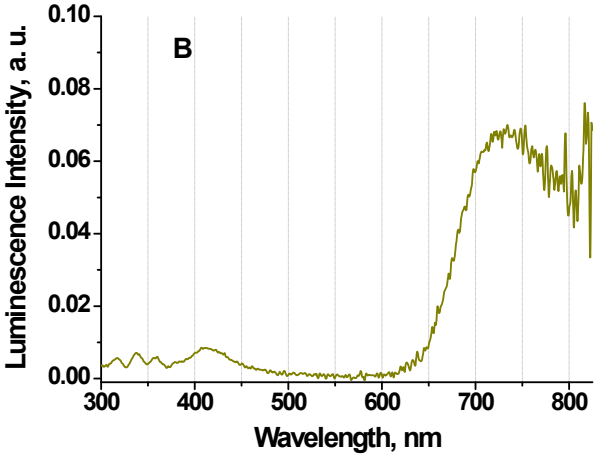

Corrected spectrum

(c) X-ray-induced luminescence of **6**

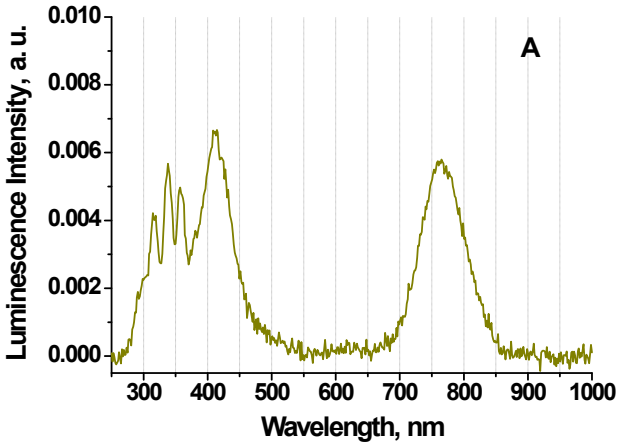

Uncorrected spectrum

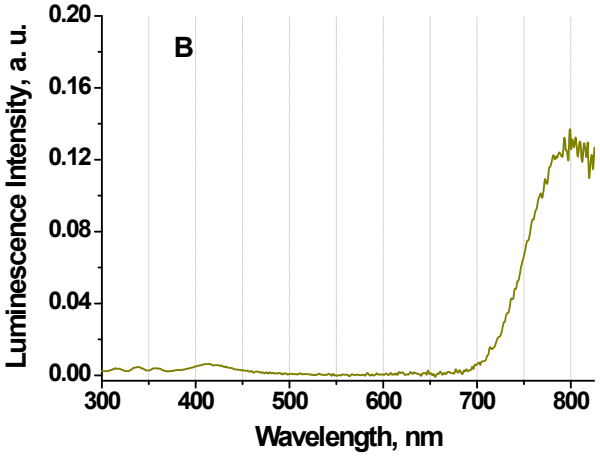

Corrected spectrum

Figure S8. Raw X-ray luminescence spectra with only baseline correction and normalization per mole of sample compound before correction for spectral sensitivity (panel A in each pair) and after applying the correction (panel B) for the **2** (a), **4** (b) and **6** (c). Spectra from panels B were used to prepare Figure 4 in the main text. The group of lines straddling the region of 400 nm is the parasitic signal from Scotch tape employed in sample mounting, which falls in the spectral range of maximum detector sensitivity and is thus rather prominent for weakly emitting complexes. Correction for spectral sensitivity curve of the detector significantly boosts the red tail of the experimental spectra containing the sought signal and turns this parasitic contribution into a rather benign artifact. No measures were taken to remove it from the spectra.

(a) X-ray-induced luminescence of **2** after ~12 hours of X-ray exposition

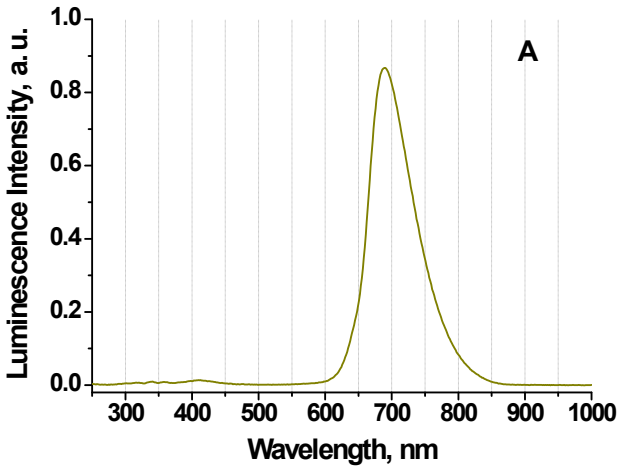

Uncorrected spectrum

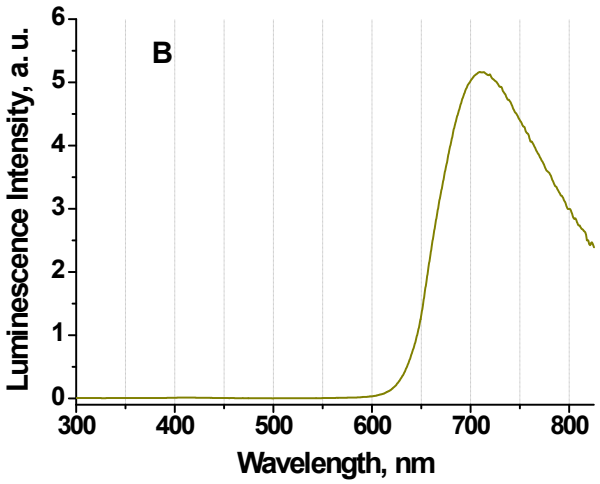

Corrected spectrum

(b) X-ray-induced luminescence of **4** after ~12 hours of X-ray exposition

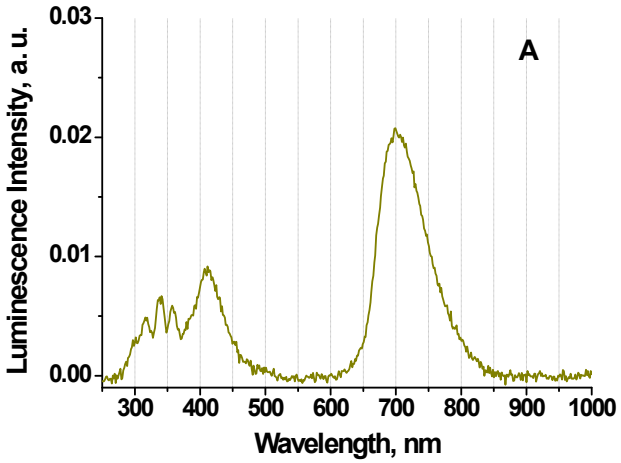

Uncorrected spectrum

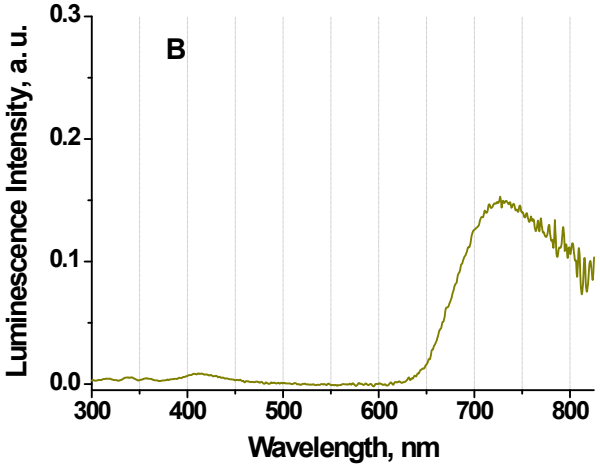

Corrected spectrum

(c) X-ray-induced luminescence of **6** after ~12 hours of X-ray exposition

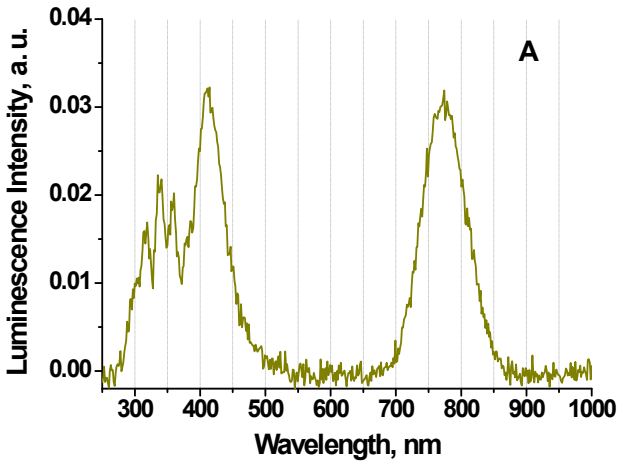

Uncorrected spectrum

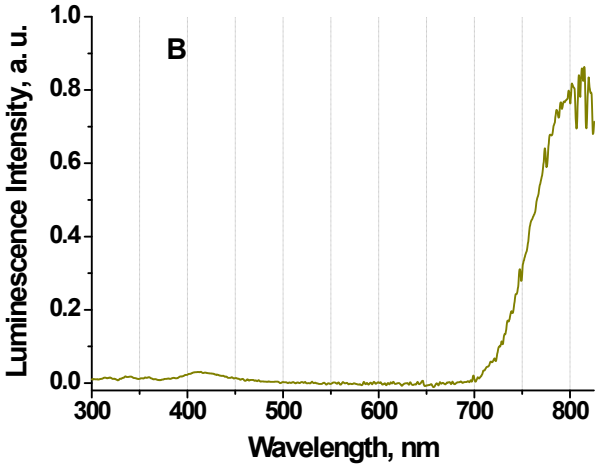

Corrected spectrum

Figure S9. Stability check: spectra reported in the main text and shown in Figure S8 took about 12 hours of X-ray exposition time each, which could potentially damage the compounds and induce luminescence centers other than clusters themselves. Samples of **2** (a), **4** (b) and **6** (c) were exposed for the same duration to collect the same dose and then the irradiated powders were checked for their chemical identity/purity: fresh samples were prepared from them and express-studied for their X-ray induced luminescence. The results, presented here in the same format as in Figure S8, are identical to the first run of spectra collected in the course of extended exposition. This strongly suggests that the observed emission is a genuine property

of the complexes themselves, although the possibility that, e.g., certain luminescent centers are induced in thin surface layer in an amount that is too small for detection via bulk chemical/structural methods, cannot yet be completely excluded.

Illustration of the possible difference in the emission spectra from interacting luminophores in the neat solid and the same luminophores in a solution using the well-known example of anthracene to stress the point that collective exciton-related spectra in the solid can be rather different from the spectra of individual molecules in a solution, provided that electronic interaction is possible between the emitting molecules in the solid. The figures show the spectra of X-ray-induced luminescence and photoluminescence for neat anthracene and for its solution in *n*-dodecane: the type of excitation can be seen to be not important, while the spectra in the neat solid and in a dilute solution are markedly different.

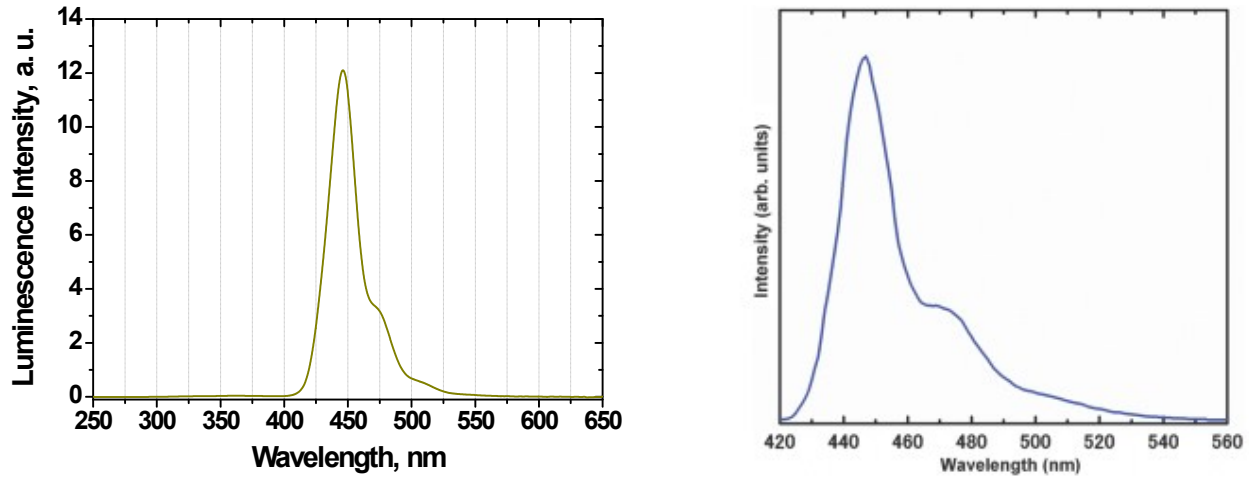

(a) (b)

Figure S10. a) Luminescence of neat solid anthracene under X-ray excitation in the conditions of the above presented experiments with hexarhenium cluster complexes; b) photoexcited (by 375 nm) luminescence of the solid anthracene (the spectrum was taken from Selvakumar, S.; Sivaji, K.; Arulchakkaravarthi, A.; Sankar, S. Electron momentum distribution and singlet-singlet annihilation in the organic anthracene molecular crystals using positron 2D-acar and fluorescence spectroscopy. *Phys. Chem. Chem. Phys.* **2014**, *16*, 15934-15940).

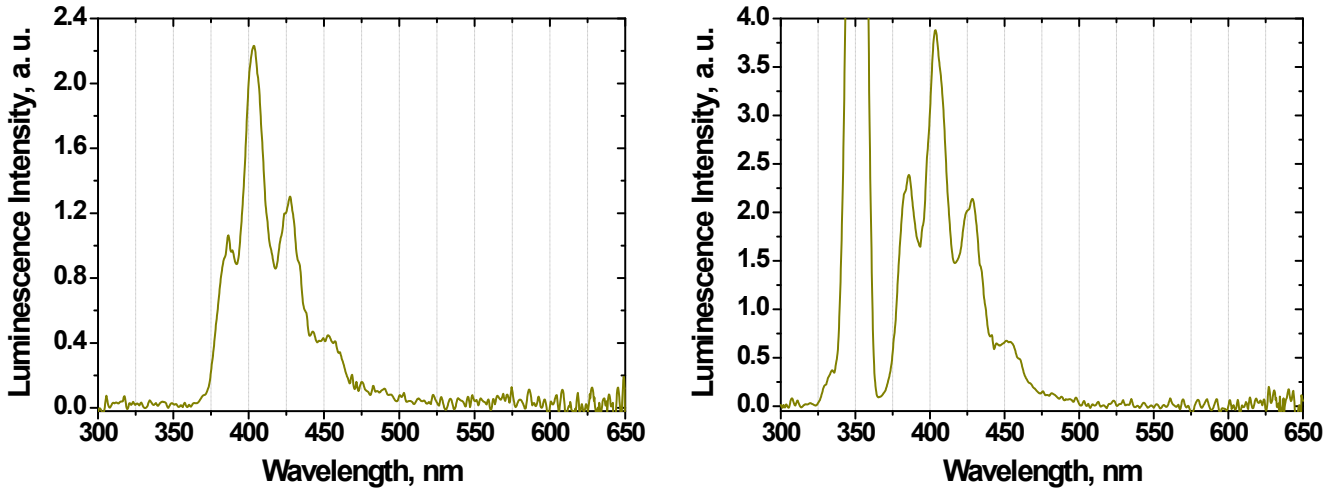

(a) (b)

Figure S11. Luminescence of solution anthracene in *n*-dodecane under X-ray excitation (a) and under photoexcitation at 345 nm (b).

(a) X-ray-induced luminescence of **1**

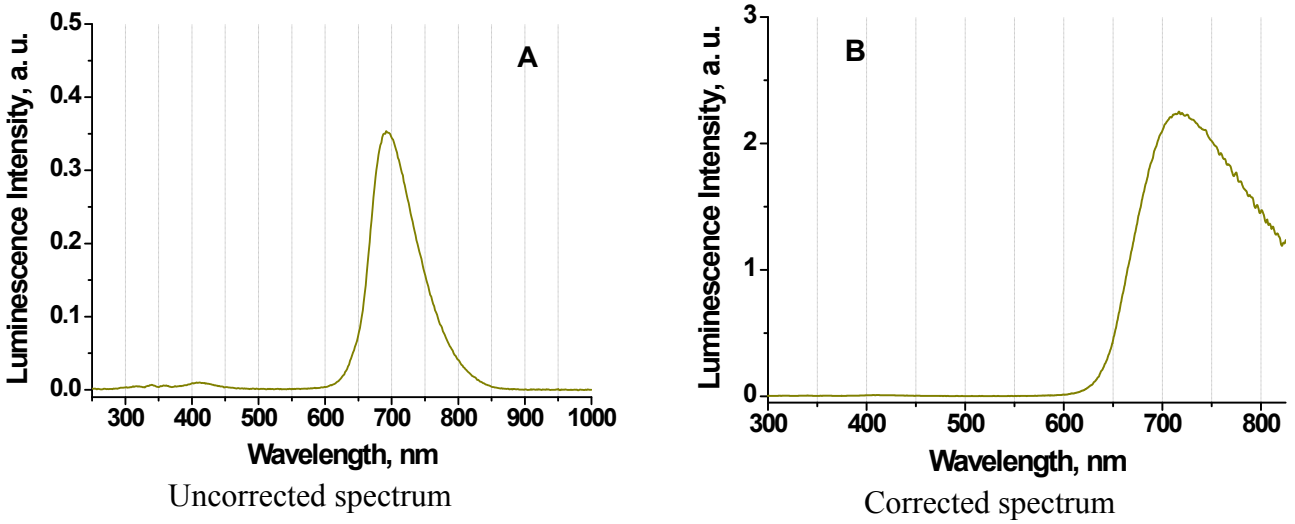

Uncorrected spectrum Corrected spectrum

(b) X-ray-induced luminescence of **3**

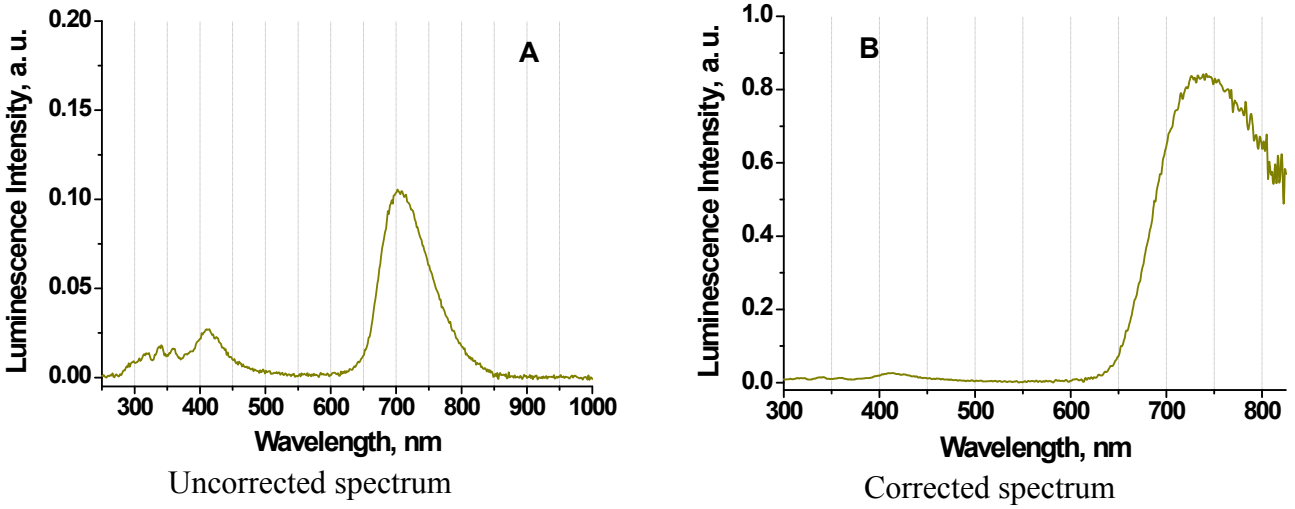

Uncorrected spectrum Corrected spectrum

(c) X-ray-induced luminescence of **5**

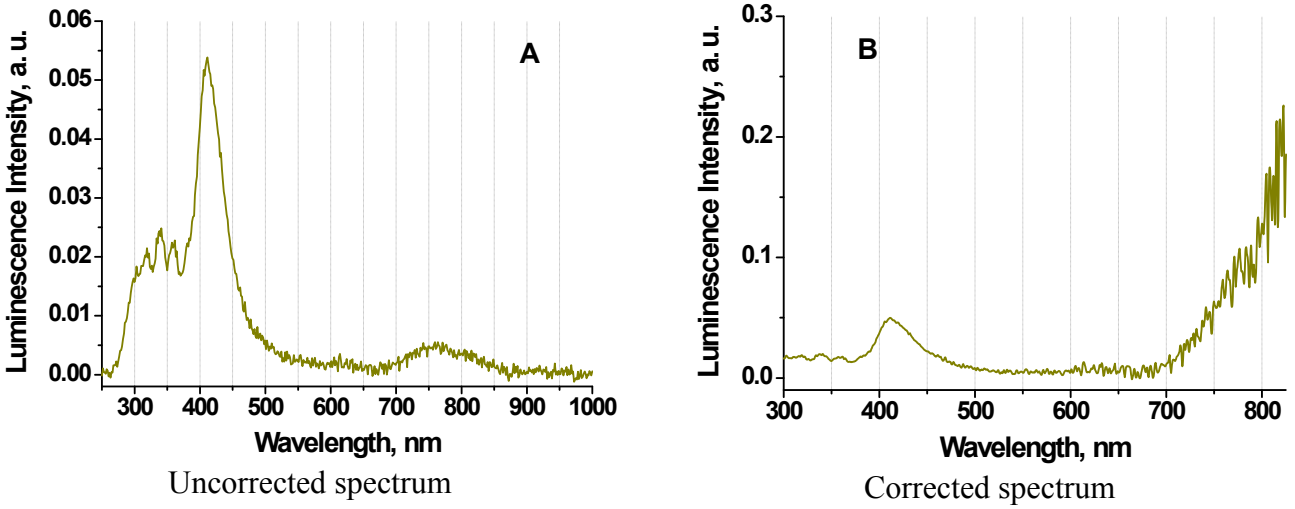

Uncorrected spectrum Corrected spectrum

Figure S12. Does the exchange of counterion influence on X-ray-induced luminescence of Re_6 cluster compound? Preliminary data demonstrated that the spectra of X-ray induced luminescence for some of the studied complexes are somewhat shifted to the red as compared to their spectra of photoluminescence in solution, which may be a sign of the effect of close neighborhood of clusters to each other in neat solid and/or of the effect of the counter-anion, both indicative of the electronic lability of the clusters. To check

whether the specific anion identity might play any role, the triflate anions of the original complexes were substituted for tetrafluoroborates, and the X-ray induced luminescence spectra from these complexes (compounds **1** (a), **3** (b) and **5** (c)) were taken and compared to the presented in Figure S8 spectra of **2**, **4** and **6**, respectively. The results obtained demonstrate that the positions and shapes of emission spectra did not change, while the relative intensities were somewhat different. This supports that the cluster cation is the emitter in these systems, and indeed indicates a possible effect of the anion in partially allowing the forbidden d–d transitions in the transition metal based cluster.